nature reviews physics

https://doi.org/10.1038/s42254-025-00836-2

Review article

Check for updates

Topological rainbow trapping

Sayed El. Soliman[1,2], Maria Barlou[3], Zi Jing Wong[1] & Kosmas L. Tsakmakidis[3]

Abstract

Topological rainbow trapping (TRT) arises from the interplay between topological states and frequency-dependent slow-wave effects. Waves first slow down, then become spatially separated by frequency and are ultimately trapped at distinct locations. TRT designs have been primarily explored in the context of photonic crystals and subsequently extended to acoustic and elastic systems. This emerging TRT concept enables robust, frequency-selective localization beyond conventional rainbow trapping, supporting compact, multi-wavelength, topologically protected platforms for extreme wave manipulation. In this Review, we elucidate the fundamental principles of TRT, emphasizing the physical mechanisms that create near-zero group velocity points with robust frequency-dependent localization. We highlight three key TRT mechanisms: graded index profiles, which gradually vary material parameters to reshape dispersion and induce slow-wave effects; higher-order topological corner modes, which exploit localized corner states for robust frequency-specific wave confinement; and synthetic dimensions, which expand the parameter space of the system to engineer stable interface states at distinct frequencies. Furthermore, we address key challenges in TRT, such as energy dissipation and tunability, while highlighting its broad range of potential applications. Finally, we discuss emerging research directions for TRT.

Sections

[1]School of Electronic Science and Technology, Eastern Institute of Technology, Ningbo, Zhejiang, China. [2]Physics Department, Faculty of Science, Assiut University, Assiut, Egypt. [3]Section of Condensed Matter Physics, National and Kapodistrian University of Athens, Panepistimioupolis, Athens, Greece. e-mail: zijing@eitech.edu.cn; ktsakmakidis@phys.uoa.gr

Key points

- Topological rainbow trapping (TRT) combines slow-wave effects with topological protection to achieve robust, frequency-selective localization in photonic, acoustic and elastic systems.

- TRT relies on Berry curvature, which induces anomalous velocity that reshapes wavepacket dynamics and enables near-zero group velocity localization through either external gradients or intrinsic band structure engineering via topological invariants.

- Graded index profiles, higher-order topological corner modes and synthetic dimensions are key mechanisms that facilitate the realization of TRT.

- Advances in complex-frequency excitations enable dynamic tunability and loss mitigation, potentially extending TRT to ultrafast, reconfigurable and broadband wave-based devices.

- Future research directions include integration with plasmonics, quantum optics and inverse design, which could open new platforms for tunable, broadband and adaptive wave control.

Introduction

Rainbow trapping describes a phenomenon in which waves spanning a broad range of frequencies are simultaneously decelerated or stopped within a linear, time-invariant system. Each frequency component is localized at a distinct spatial position, a process known as spatial demultiplexing. Rainbow trapping can be achieved in guiding structures whose widths vary adiabatically, either linearly or in other functional forms, along the propagation direction. Although it was initially proposed for electromagnetic waves[1], rainbow trapping has been generalized and demonstrated across various wave types, including acoustic[2], elastic[3], mechanical[4], water[5] and seismic[6] waves. For each type of wave, the phenomenon can usually be observed in two classes of structures, which are defined by the size of the structural elements relative to the operating wavelength.

Plasmonic and metamaterial structures rely on unit elements that are considerably smaller than the wavelength. In these cases, rainbow trapping is achieved by designing materials with contrasting material parameters (for electromagnetic waves, the refractive index or the permittivity) that induce opposite power flows in different regions, which ultimately reduces the energy velocity, even to zero, resulting in strong wave confinement (Fig. 1a). Similarly, graded subwavelength structures with spatially varying width or depth can also modify local dispersion, enabling frequency localization at distinct positions. The second option is periodic structures, such as photonic, acoustic and elastic crystals with periodic elements on the order of the operating wavelength. In these structures, rainbow trapping occurs through Bragg scattering and material dispersion. Chirped, graded or tapered periodic geometries can modify the band structure to flatten the dispersion curve, causing the group velocity $v_g = d\omega/dk$ to approach zero at specific points (Fig. 1c). This mechanism is responsible for slow-wave states[7–9] and enables frequency-dependent spatial localization, which is a key feature of rainbow trapping.

Although rainbow trapping offers an effective method for wave control, its performance can be sensitive to structural imperfections and fabrication errors. This challenge has inspired researchers to explore more robust wave manipulation mechanisms, including topological photonics[10–12]. Topological photonics leverages concepts from a branch of mathematics that deals with properties of structures invariant under continuous deformation to engineer optical materials and structures with remarkable robustness against defects[13–15]. By integrating topological concepts into photonic systems, researchers have realized phenomena, including robust edge[16–18] and corner states[19–21], topological phase transitions[22–24] and non-reciprocal propagation of light[25–27]. Such phenomena provide a method to create optical systems that are inherently resilient to defects and disorder, which facilitates efficient and reliable wave transport[28–30].

At the core of topological photonics is the Berry curvature — a fundamental geometric property of Bloch bands that significantly influences wave propagation dynamics, modifies group velocity and enables robust slow-light effects. Understanding this topological influence extends traditional rainbow trapping into the framework of topological rainbow trapping (TRT).

In photonic crystals (PCs), the periodic modulation of the refractive index creates band structures analogous to electronic systems. The geometric properties of Bloch eigenstates are described by the Berry connection $\mathcal{A}_n(k) = i\langle u_{nk}|\nabla_k| u_{nk}\rangle$ and Berry curvature $\Omega_n(k) = \nabla_k \times \mathcal{A}_n(k)$, in which u_{nk} represents the periodic part of the Bloch function for the nth band[31,32]. This curvature acts as an effective magnetic field in momentum space that alters photon dynamics. Integrating the Berry curvature over the entire Brillouin zone (BZ) yields the Chern number, $C_n = \frac{1}{2\pi}\int_{BZ}\Omega_n(k)d^2k$ (ref. 33). A non-zero Chern number (topological invariant) indicates the presence of robust, unidirectional topological edge states, which are immune to backscattering caused by structural imperfections[28,34,35].

Berry curvature introduces an anomalous velocity term into the semiclassical equations governing electron dynamics. This effect was first identified in ref. 36 and has since been extensively studied across a range of physical systems, including magnetic Bloch bands[37], ultracold gases[38], liquid crystal microcavity with 2D perovskite[39] and non-Hermitian systems under complex electric fields[40]. The resulting group velocity correction can be expressed as $v_n(k) = \nabla_k E_n(k) - eE \times \Omega_n(k)$, in which $E_n(k)$ is the energy dispersion, $E = -\nabla V(r)$ represents the externally applied electric field and eE represents the resulting force. The first term $\nabla_k E_n(k)$ describes the conventional group velocity in periodic systems, whereas the second term $-eE \times \Omega_n(k)$ reflects the anomalous velocity from Berry curvature $\Omega_n(k)$, whose orientation is transverse to the applied field[31,41,42]. This anomalous velocity becomes pronounced near band extrema or in regions with strong Berry curvature, which strongly influences transport behaviour[43]. Such conditions have been explored in electronic phenomena, including the anomalous Hall effect[44,45] and spin Hall effect[46], which fundamentally alter transport dynamics[31], and in systems subject to strain gradients or structural modifications[47,48]. An analogous anomalous velocity correction has also been observed in optical media[49], where it manifests as a velocity component perpendicular to refractive index gradients[41,50].

In topological PCs, the group velocity equation follows an analogous form: $v_g = \nabla_k \omega(k) + \Omega(k) \times \nabla_r V_{ext}(r)$, in which $\omega(k)$ is the photonic dispersion relation, and $V_{ext}(r)$ represents external perturbations such as refractive index gradients or electromagnetic field profiles. This correction reflects the influence of the Berry curvature on wave dynamics, mirroring the behaviour in electronic systems. By carefully engineering Berry curvature distribution in a topological photonic system, one can modify the dispersion relation from $\omega(k)$ to $\omega(k) + \Omega(k)$, thereby manipulating

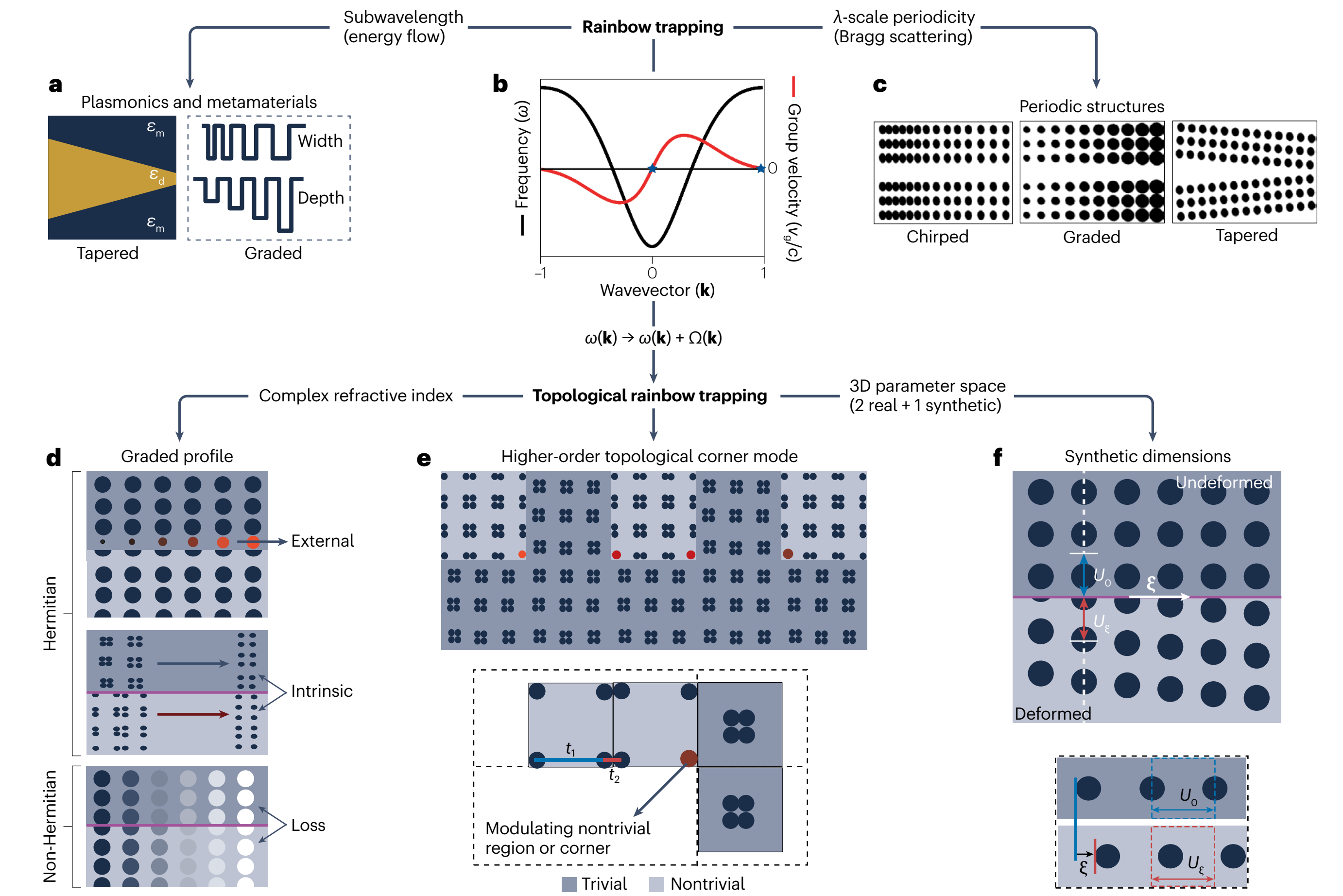

Fig. 1 | From rainbow trapping to topological rainbow trapping. a, In tapered plasmonic structures, rainbow trapping is achieved by engineering opposite-sign permittivity in metals (ε_m) and dielectrics (ε_d) to induce counter-propagating power flows while gradually varying the geometry to reduce the net energy velocity and spatially localize different frequencies. In graded subwavelength metamaterials, spatially varying width or depth of the unit elements modifies local dispersion, which enables multiple slow-light modes to form at distinct frequencies and trapping positions. **b**, The dispersion relation highlights frequency-dependent wave trapping at points of near-zero group velocity. Incorporating Berry curvature modifies dispersion as $\omega(\mathbf{k}) \to \omega(\mathbf{k}) + \Omega(k)$, creating topologically robust, frequency-selective trapped states. Blue stars denote near-zero velocity points crucial for localization. **c**, Rainbow trapping in periodic structures (photonic, acoustic and elastic) relies on Bragg scattering. Chirped, graded or tapered lattice geometries spatially modulate the dispersion, creating slow-wave states and enabling frequency separation. **d**, Topological rainbow trapping (TRT) realized via graded index profiles. In Hermitian systems (top and middle panels), external gradients are introduced at a pre-existing topological interface to reshape local dispersion, whereas intrinsic gradients arise directly from the topological band structure without requiring external perturbations. In non-Hermitian systems (bottom panel), spatial variations in the imaginary part of the refractive index introduce graded loss profiles that similarly control dispersion and enhance spatial localization. **e**, TRT realized via higher-order topological corner modes. Frequency-specific localization occurs at spatially separated cavities (corners) by modulating intra-cell (t_1) and inter-cell (t_2) coupling strengths or by local geometric corners deformation, forming a discretized robust rainbow. **f**, TRT realized using synthetic dimensions. Introducing an additional synthetic parameter ξ (unit-cell displacement from undeformed U_0 to deformed U_ξ) expands the 2D parameter space to a 3D parameter space (two spatial dimensions and one synthetic dimension), enabling robust, frequency-dependent interface states without requiring physical refractive index gradients.

the effective group velocity, and achieve conditions similar to flat-band behaviour, corresponding to near-zero group velocity (Fig. 1b). Although Berry curvature may not always flatten the band directly, it introduces an anomalous velocity term that can create a near-zero effective velocity even in systems without inherently flat bands. This mechanism offers new possibilities to confine light, enhance slow-light effects and improve energy localization in photonic structures.

TRT is a concept that merges the robustness of topological photonics[51–53] with efficient frequency separation and slow-wave effects[54–56]. Unlike traditional rainbow trapping, which relies on material or geometric dispersion shaping and is often sensitive to disorder, TRT leverages topological invariants, such as the Chern number, to design band structures that support zero-group velocity states, ensuring robust and spectrally multiplexed localization immune to fabrication imperfections. Early studies are primarily focused on theoretical designs and proof-of-concept demonstrations of TRT in photonic platforms[57,58]. However, the field has rapidly evolved, with recent experimental studies extending TRT across diverse wave-based systems from PCs[59–61] to acoustic[62–64], elastic[65–67] and non-Hermitian media[68]. Additionally, there is an emerging trend to move TRT from passive dispersion control to active, tunable and integrated devices.

TRT is achieved by spatially varying a parameter that induces a topological phase transition, such as refractive index profile, unit-cell geometry or coupling strength, which creates a continuous gradient of interface states. Each of these topological interface states is pinned to a distinct spatial location, forming a stable 'topological rainbow', in which individual frequency components are localized at specific positions along the interface[57,62,69,70]. This mechanism relies on regions that are engineered to have distinct topological properties, which enables frequency-selective trapping through controlled topological bandgap modulation. As the topologically protected modes are guaranteed by the underlying topological invariants, these localized states are inherently robust against structural imperfections, backscattering and environmental disturbances.

This Review provides a comprehensive overview of the fundamental principles of TRT, with a focus on the topological mechanisms that enable its formation. We explore how graded index profiles, higher-order topological corner states and synthetic dimensions contribute to the realization of TRT, particularly in PCs, and extend the discussion to acoustic and elastic wave systems. Additionally, we address key challenges related to energy dissipation and tunability, highlighting recent advancements aimed to overcome these limitations. This Review also seeks to establish the potential of TRT in optical information processing, energy harvesting and next-generation wave-based sensing and computing technologies.

Design principles for TRT

As highlighted in Fig. 1, TRT can be realized through various strategies, each based on different physical mechanisms. Broadly, TRT emerges through two distinct pathways that combine topological protection with slow-light effects. The following section discusses these two design pathways in detail.

Introducing the slow-light rainbow effect into structures with topological states

The slow-light rainbow effect can be introduced to systems that already support topologically protected states by applying external gradients, such as graded refractive index profiles, material inhomogeneities or geometric tapering. These gradients reshape the local dispersion, leading to points with near-zero group velocity at which specific frequency components become spatially localized. Although the topological states enhance robustness, the slow-light behaviour itself arises from the engineered gradient rather than from intrinsic topological features. Thus, the resulting frequency-dependent localization can be called a topological trapped rainbow, which is supported by robust interface modes.

This approach offers a relatively straightforward and flexible design route. However, it comes with certain trade-offs: the length of the gradient region limits how many frequencies can be spatially resolved, and steep gradients may break adiabaticity, leading to scattering or incomplete trapping. Furthermore, if the refractive index modulation pushes the localized states near the bandgap edge, it can introduce coupling with bulk modes or induce non-topological backscattering. Therefore, careful design is essential to ensure robust frequency-selective localization while preserving the topological phase.

Designing a topological state with a slow-light rainbow effect

The alternative design pathway to achieving TRT is to engineer the topological properties themselves to induce a slow-light rainbow effect that arises intrinsically from the band structure. In this scenario, topological invariants govern the group velocity, allowing zero-group velocity points to form naturally without the need to introduce external gradients. The dispersion is modified directly through its topological design, enabling different frequencies to localize at distinct spatial positions, forming a pure topological trapped rainbow.

A representative example involves topological insulator heterostructures, in which domain walls between regions with different structural parameters, although not necessarily different Chern numbers, support continuously shifting localized edge states in a single bandgap. These states exhibit frequency-dependent confinement while retaining topological protection as long as the bandgap remains open. A related mechanism was demonstrated in ferrimagnetic PCs, in which multiple Dirac and quadratic degeneracies were lifted to produce a bandgap and generate non-zero Chern numbers. The associated Berry flux contributions are added constructively, which increases the net Chern number[53,71,72]. In such systems, spatially varying the Chern number by creating domain walls between regions with distinct topological phases forms heterostructures that support frequency-dependent edge states. Although this also enables frequency separation, TRT achieves a more continuous and robust frequency gradient by guiding localized modes within a single, unbroken topological phase without requiring multiple bandgaps or Chern number transitions.

In summary, both design principles can realize TRT, but the latter, based on intrinsic topological design, offers a more fundamental and robust path to efficient slow-light behaviour without introducing external structural perturbations. Crucially, because these trapped modes are topological in origin, they are highly resistant to scattering and disorder. This protection ensures that, as long as the bandgap remains open and the topological phase is preserved, the trapped modes remain decoupled from radiative or bulk propagating states. Both strategies enable the design of TRT across photonic, acoustic and elastic systems.

TRT in photonic crystals

One of the most widely used platforms to design and realize TRT is PCs, which leverages the interplay between topologically protected states and spatially modulated dispersion. In PCs, the periodic variations of the refractive index lead to the formation of photonic band structures[73]. The electric field satisfies the Bloch wave condition, resulting in a dispersion relation $\omega(k)$ that defines the group velocity and energy flow. By introducing gradual variations in refractive index or unit-cell geometry, the local dispersion can be systematically tuned, creating spatial regions where the group velocity approaches zero. This enables effective light trapping at well-defined positions within the structure. In the following sections, we discuss key mechanisms to achieve TRT in PCs, including the use of graded index profiles, higher-order topological corner modes (HOTCMs) and synthetic dimensions.

Graded index profiles

In Hermitian systems, introducing an external or intrinsic gradient such as a spatially varying refractive index can reshape the local dispersion, forming controlled slow-light regions (Fig. 1d, top and middle panels). TRT can be realized by incorporating graded index profiles, commonly done through gradual variation of material parameters such as refractive index[74–76], density[77,78] or stiffness[66,69,79] along the propagation direction. Such gradual variation alters the local dispersion relation, progressively reducing the group velocity for different frequency components and enabling their spatial separation. Unlike abrupt structural discontinuities, these adiabatic transitions suppress scattering and minimize energy losses. When integrated with topological states, graded profiles support stable wave confinement that is immune to defects. Berry curvature can further enhance this effect by manipulating the effective group velocity and achieving conditions similar to flat-band behaviour, thereby improving frequency-dependent localization.

In PCs, graded profiles are typically implemented through gradual variations in refractive index or lattice geometry. One notable example involves introducing controlled contractions and expansions across trivial and nontrivial regions to tune the dispersion characteristics and to enable TRT[80], as shown in Fig. 2a. This deformation leads to the opening of doubly degenerate Dirac cones and the emergence of topological edge states. In this case, the built-in gradient of the system reshapes the local band structure and controls the group velocity without relying on external gradients, resulting in the frequency-dependent localization of spectral components at distinct spatial positions. This approach has largely been explored through numerical simulations. For example, simulations of all-dielectric triangular-lattice PCs demonstrated robust state confinement over $0.6358-0.6517\,c/a$ (in which c is the speed of light and a is the lattice constant, and c/a denotes the normalized frequency) with spatially separated trapping across the graded structure.

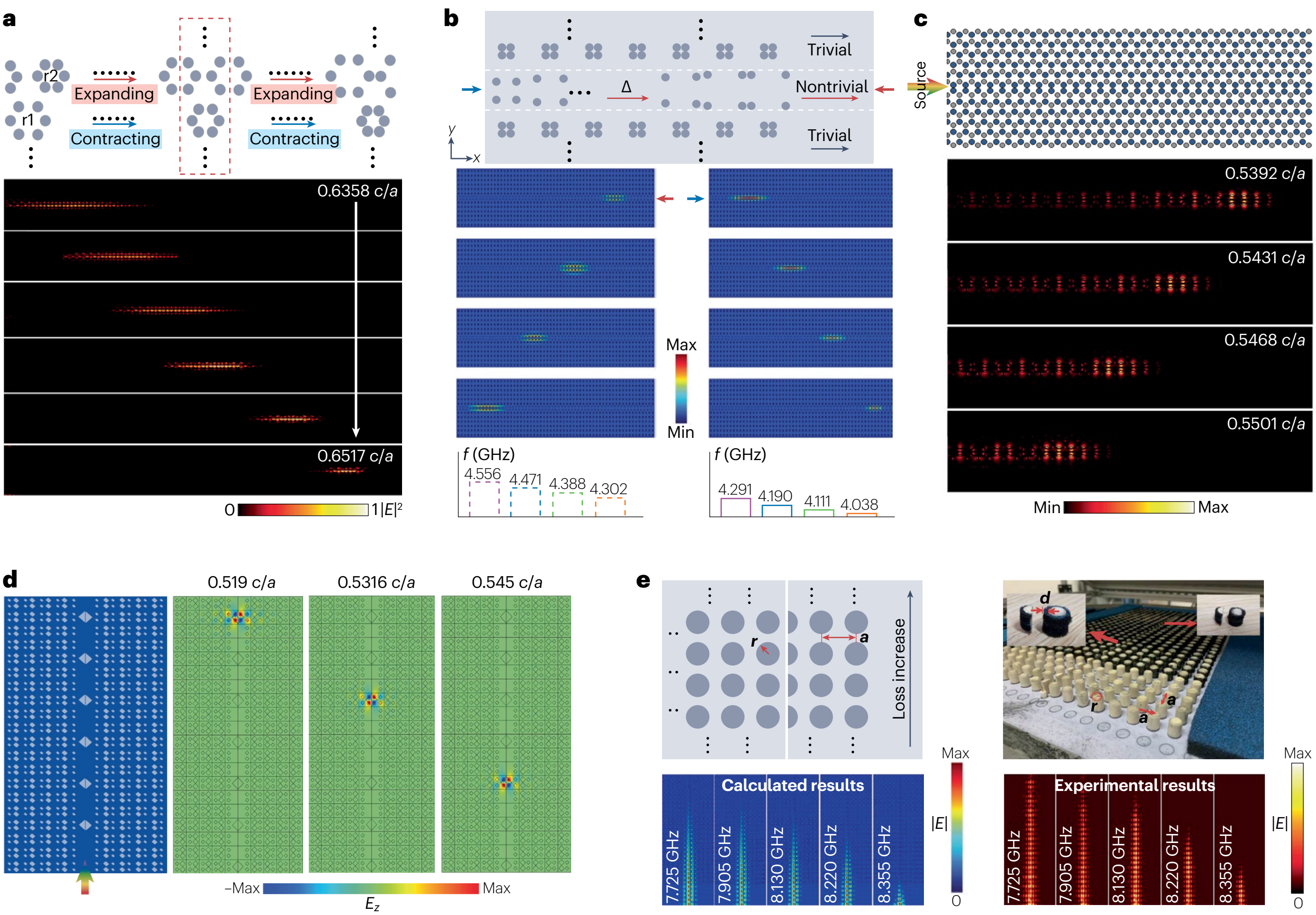

Fig. 2 | Photonic topological rainbow trapping based on graded index profiles. a, Schematic of a graded topological photonic crystal (PC) formed by combining expanded and contracted lattice regions. The resulting refractive index gradient induces topological edge states and frequency-selective confinement. Frequencies are labelled as normalized c/a, and $|E|^2$ denotes the normalized electric field intensity distribution. Adapted with permission from ref. 80, Optica Publishing Group. **b**, Trivial–nontrivial–trivial PC heterostructure with C_4-symmetric unit cells, enabling dual-mode topological rainbow trapping (TRT). The central region is modified via a geometric tuning parameter Δ applied along both the x and y coordinates, inducing geometric deformation between unit cells. The corresponding electric field $|E|$ distribution illustrates trapped odd (left) and even (right) coupled topological edge states with different frequencies given in the corresponding positions at the bottom. Reprinted with permission from ref. 81, IOP. **c**, Gradient valley PC with spatially varying graded domain along the interface, demonstrating frequency-dependent localization via valley-locked edge states and controlled group velocities. Adapted with permission from ref. 82, Optica Publishing Group. **d**, Quadrupole TRT modes are achieved by varying cavity length along a topological waveguide interface. Simulated out-of-plane electric field (E_z) distributions verify that the external cavity gradient induces robust light trapping at multiple frequencies. Adapted with permission from ref. 83, Optica Publishing Group. **e**, Non-Hermitian TRT in a PC with spatially graded loss. The parameter d denotes the thickness of the lossy electromagnetic shielding material wrapped around dielectric cylinders to vary the local loss profile. Both simulation and experiment confirm that controlled loss gradients enable wave localization across multiple frequencies. Adapted with permission from ref. 68, Chinese Laser Press.

Another example studied through simulations involves a trivial–nontrivial–trivial heterostructure with C_4-symmetric unit cells, in which the gradual tuning of the central region enabled TRT via odd and even coupled topological edge states[81] (Fig. 2b). This dual-frequency TRT covered 4.038 − 4.556 GHz, with each mode selectively confined at distinct spatial locations within the same graded interface. In a related approach, a gradient valley PC was designed using asymmetric dielectric rods of relative permittivity ($\varepsilon = 12$) to control group velocity and valley dispersion along the interface, enabling frequency-selective localization via valley-locked edge states[82] (Fig. 2c). This theoretical study demonstrated TRT over the frequency range 0.5392 − 0.5501c/a, with spatially separated valley modes confined along the graded domain.

TRT can also be induced through cavity-based designs. In this approach, the edge lengths of dielectric cavities are intentionally modified to create geometric defects in a periodic lattice. These defected cavity lengths are gradually varied along a topological waveguide interface[83] (Fig. 2d), introducing spatial grading that modulates coupling between neighbouring cavities and enables control over light localization and group velocity. This numerical work combined a topological waveguide with length-graded square dielectric cavities to realize dipole and quadrupole mode trapping; as cavity lengths reached $3a$ or greater, the group velocity was reduced to near zero, resulting in strong confinement and flat bands. Localized out-of-plane electric field distributions were observed at frequencies of 0.519 c/a, 0.5316 c/a and 0.545 c/a, corresponding to distinct spatial trapping. Here, the slow-light rainbow effect emerged from graded defected cavity geometries, whereas topological edge states ensured robustness. Importantly, the slow-light behaviour in this system was not an intrinsic property of the topology itself but is externally engineered through deliberate cavity length variation.

A non-Hermitian system adds an extra degree of freedom to control wave behaviour by using spatially graded loss profiles or gain–loss distributions to induce the rainbow effect[68]. In this context, the eigenstate $n_m(k_x, k_y, n_i)$ in the momentum space of the mth band is characterized by the Bloch wavevector ($\mathbf{k}_x$, $\mathbf{k}_y$) and the imaginary part of the refractive index $n_i(x)$, which defines the position-dependent loss (Fig. 1d, bottom panel). This spatial loss gradient modifies the local propagation constant and progressively reduces the group velocity of the interface mode, eventually reaching zero at specific spatial locations, thereby enabling light trapping. Although this loss-gradient mechanism can independently induce RT, a deeper understanding reveals its connection to exceptional points (EPs) and unique degeneracies in non-Hermitian systems[84,85]. An EP occurs when $\gamma = \kappa$, in which γ represents the gain or loss coefficient and κ is the coupling coefficient between the interacting modes of the system, such as coupled resonators or waveguide modes, whose interactions are influenced by spatial variations in loss or gain.

At or near an EP, the dispersion relation can be significantly modified, and under specific conditions, this may lead to a substantial reduction of group velocity, which supports light localization. By spatially grading the loss function, the EP condition shifts across different spatial locations for different frequencies, enabling the rainbow trapping effect. A recent experimental observation of TRT in non-Hermitian PCs[68] demonstrated the versatility of this approach. As shown in Fig. 2e, graded loss engineering combined with tailored dispersion played a crucial role in achieving robust frequency-selective light confinement. This study realized TRT in a non-Hermitian square-lattice PC of dielectric cylinders ($n = 2.4 + in_i$) by introducing a gradient in the imaginary refractive index across 7.725 − 8.355 GHz, with near-field microwave measurements confirming robust spatial separation of modes along the graded interface.

Higher-order topological corner modes

HOTCMs offer a robust and discretized mechanism for frequency-selective localization in TRT (Fig. 1e). In higher-order topological insulators such as breathing kagome lattices and locally resonant metamaterial plates, the band structure is governed by a tight-binding model with alternating intra-cell (t_1) and inter-cell (t_2) coupling strengths[86]. When $t_2 > t_1$, the corner states naturally emerge within the bandgap, acting as localized energy traps. For TRT, introducing spatial gradients in parameters such as coupling strength or unit-cell geometry allows these corner state eigenfrequencies to vary along the structure, resulting in a discrete topological rainbow[59,87,88]. As the group velocity of these modes approaches zero ($v_g \to 0$), different frequency components become confined at distinct spatial positions. The robustness of this localization is protected by higher-order topological invariants[89,90], such as crystalline symmetry eigenvalues or the quantized corner charge: $Q_c = \frac{1}{2\pi}\int_{BZ} A(k)\mathrm{d}k$. These invariants guarantee stability against structural disorder and imperfections[91,92], making HOTCM-based TRT highly reliable for practical applications.

A notable implementation of this concept was introduced in ref. 87, using two distinct configurations of breathing kagome PCs (K1 and K2) with different topological phases (Fig. 3a). Additionally, four perturbed kagome PCs (BK1–BK4) with C_3 symmetry were fabricated to enhance corner state formation. A polygonal layout enabled selective localization of corner states at vertices C_1–C_4. The corresponding field patterns (Fig. 3b) clearly exhibited the frequency-dependent localization associated with TRT. This work combined theoretical and experimental analysis to demonstrate discretized TRT via HOTCMs confined between 5.52 GHz and 6.26 GHz, exhibiting strong corner-localized confinement and spectral separation. Integrating tailored corner states with cavity engineering further refined the approach[88]. By geometrically modulating the sector angles of circular dielectric elements specifically at the corners of the PC heterostructure and introducing a central cavity with a defect, this simulation-based design enabled discrete topological mode localization across 0.339 − 0.398c/a (Fig. 3c). The resulting discretized rainbow exhibited robust cavity and corner mode separation with high spatial confinement. This approach offers strong structural tunability and compact implementation, enabling flexible multi-frequency TRT without external control.

More recently, HOTCM-based TRT was enhanced by leveraging spatial modulation techniques to dynamically tune gapless corner modes in PC slabs[59]. As shown in Fig. 3d, a structured design incorporating gradient and barrier regions enabled precise frequency-dependent confinement at distinct corners. This work experimentally demonstrated HOTCM-based TRT by introducing synthetic translational gradients in PC slabs composed of ceramic square rods on a metallic substrate, and near-field microwave measurements confirmed the localization of corner modes spanning 6.49 − 7.34 GHz. These results highlight the flexibility of HOTCM-based architectures for discrete frequency localization, offering high spectral resolution, and the ability to resolve frequency differences as small as 0.06 GHz, making them highly suitable for compact, frequency-multiplexed photonic devices.

Synthetic dimensions

Synthetic dimensions provide an effective way to simulate higher-dimensional physics within lower-dimensional systems. This approach introduces additional degrees of freedom such as angular momentum,

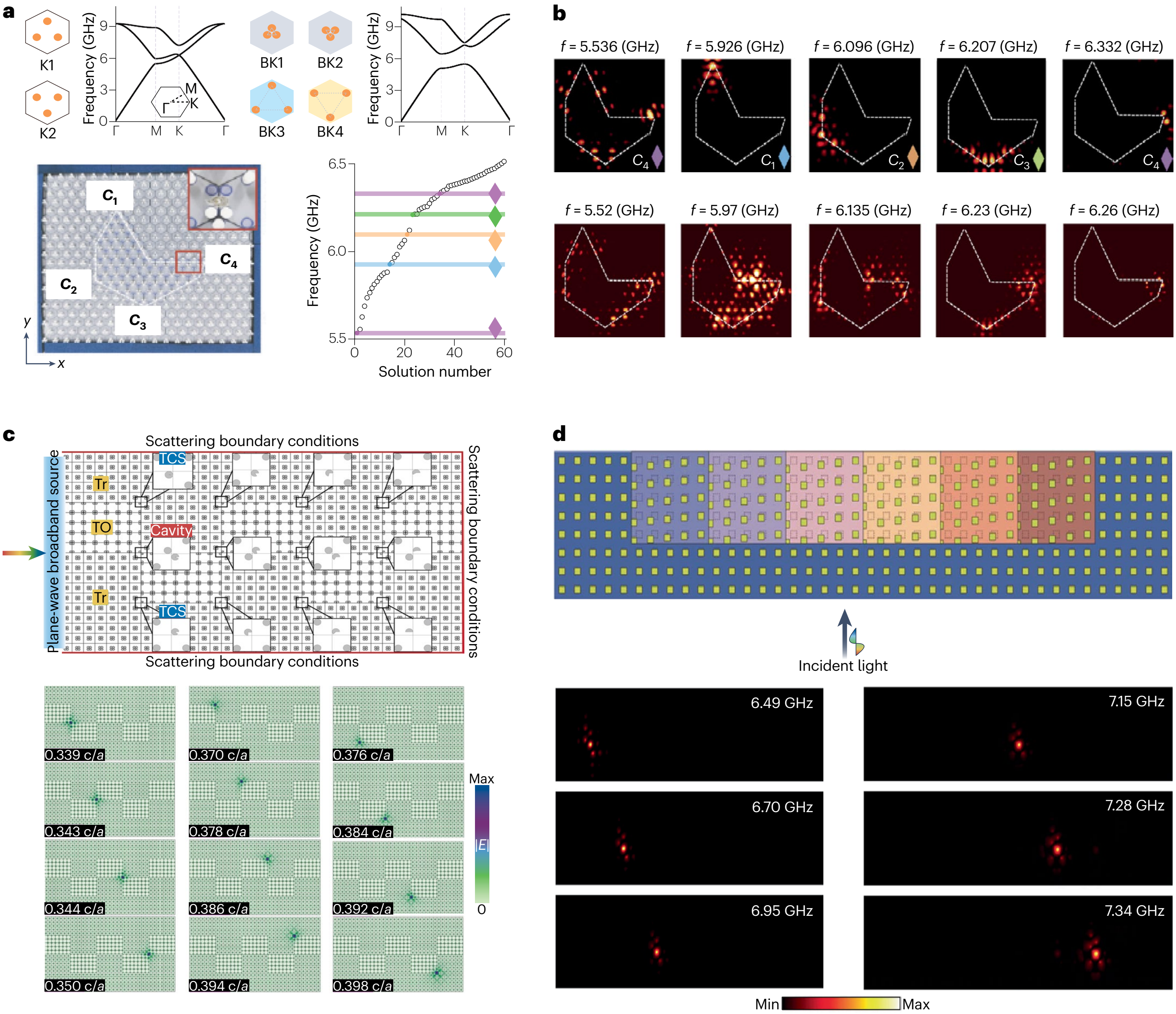

Fig. 3 | Photonic topological rainbow trapping based on higher-order topological corner modes. **a**, Band structures of unperturbed (K1, K2) and perturbed kagome photonic crystal (PC) (BK1–BK4) lattice configurations with different topological phases to induce corner localization. A polygon structure incorporating different corner types (C_1–C_4) supports distinct, localized corner modes. Adapted with permission from ref. 87, Optica Publishing Group. **b**, Calculated eigenfield (top panel) and measured field (lower panel) patterns showing higher-order topological corner modes confined to corners C_1–C_4 of the structure in part **a** at different frequencies. Adapted with permission from ref. 87, Optica Publishing Group. **c**, PC heterostructure integrating varying sector angles to tune corner and cavity geometries. Trivial (Tr) and topological (TO) regions denote the domains forming the interface for topological confinement. Multiple confined topological corner states (TCSs) form a discretized topological rainbow. Reprinted with permission from ref. 88, Wiley. **d**, Synthetic gradient introduced in PC slabs enables gapless higher-order topological corner modes to emerge across the structure. Calculated out-of-plane electric field distributions confirm frequency-separated corner localizations at specific frequencies. Adapted with permission from ref. 59, Optica Publishing Group.

frequency, phase or unit-cell displacement that expand the effective parameter space and enable precise control over wave dynamics and topological transitions[93–95]. In PCs, the dispersion relation $\omega(k)$ typically resides in a 2D parameter space defined by the Bloch wavevector (k_x, k_y). Adding a synthetic translational parameter ξ, such as a continuous shift in unit-cell position, expands this to a 3D parameter space (k_x, k_y, ξ), that is, two real and one synthetic dimension (Fig. 1f). Within this extended parameter space, nontrivial topological effects arise, characterized by the Zak phase (θ_n^{Zak}) and Chern number $C_n(k_y)$, defined as[58]:

$$C_n(k_y) = \frac{1}{2\pi}\int_{-a/2}^{a/2} \frac{\partial\theta_n^{\mathrm{Zak}}(k_y,\xi)}{\partial\xi}d\xi.$$

Gradually varying the displacement parameter ξ across the structure modulates the Zak phase continuously, leading to topologically nontrivial bands and robust interface states at different frequencies. These states exhibit near-zero group velocity ($v_g \to 0$), enabling TRT without requiring any physical gradient in refractive index or geometry.

An early theoretical demonstration of TRT using synthetic dimensions was reported in ref. 58, in which a synthetic spatial parameter ξ, implemented via tapered unit-cell geometry, was used to create TRT in a 2D PC (Fig. 4a). Spatial modulation of ξ induced band topology characterized by a Chern number, enabling robust interface states spanning 0.343 − 0.3775c/a with minimal mode overlap and sharply localized field confinement. Unlike gradient-based systems, this approach inherently produced slow-light behaviour through topological design, eliminating the need for external gradient engineering. Tuning the synthetic parameter localized distinct frequency components at different spatial positions, forming a topological rainbow. This method is highly versatile, as it is independent of specific symmetries, lattice structures, material properties and wavelength ranges.

Notably, TRT based on synthetic dimensions has been extended to lossy systems[96], preserving robustness even in non-ideal environments, as shown in Fig. 4b. This numerical study used a non-Hermitian twisted PC to realize TRT through tunable interface states spanning 0.475 − 0.5183c/a. Frequency selectivity was achieved by modulating material loss, enabling robust confinement even in the presence of energy dissipation. The first experimental demonstration of nanoscale

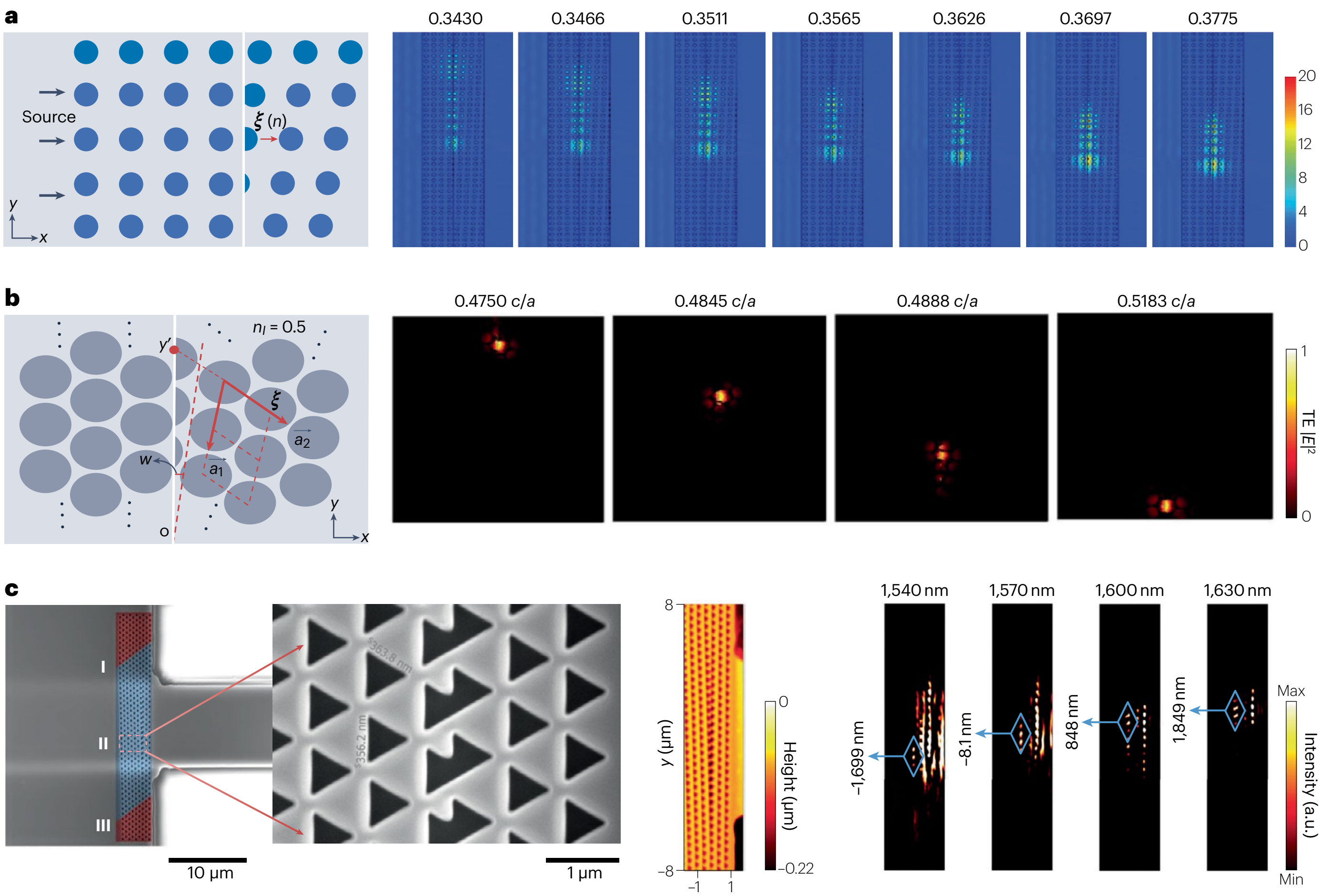

Fig. 4 | Photonic topological rainbow trapping based on synthetic dimension. **a**, Topological rainbow trapping is realized by introducing a synthetic dimension through unit-cell deformation. The synthetic parameter $\xi(n)$, representing the translational deformation of the nth unit cell, continuously tunes the topological state, resulting in slow-light and frequency-dependent localization at distinct spatial positions. Right panel shows the electric field intensity distribution at different normalized frequencies (c/a). Adapted with permission from ref. 58. Copyrighted by the American Physical Society. **b**, A theoretical model of a photonic crystal implementing a synthetic parameter through lattice tapering. The point labelled 'o' marks the origin of the y-axis and the centre of rotation. The location 'y'' indicates where the air hole intersects the y-axis. The parameter w is the twisted angle, and n_i = 0.5 denotes the imaginary part of the refractive index to model non-Hermiticity. Transverse electric (TE)-polarized normalized electric field intensity $|E|^2$ distributions show the formation of highly concentrated modes at different positions along the interface at distinct frequencies. Adapted with permission from ref. 96, Optica Publishing Group. **c**, Nanoscale demonstration of a topological rainbow trapping device on a silicon-on-insulator platform. The geometric structure consists of three regions. Region II (blue) is the region responsible for frequency-dependent spatial separation of topological states owing to the nontrivial topology in synthetic dimension. Regions I and III (red) are barrier regions, which prevent the leakage of light. The central panels show the scanning electron microscopic image highlighting the triangular hole pattern, and the atomic force microscope height profile confirming the fabricated structure after etching. Measured electric field intensity distributions (right) confirm spatial separation of topological states at different wavelengths. Reprinted from ref. 97, CC BY 4.0.

on-chip TRT was realized in ref. 97 using a PC waveguide with engineered synthetic dispersion. As shown in Fig. 4c, wavelength components were selectively separated and localized within a compact silicon-on-insulator structure, in which translational deformation served as a synthetic dimension. The localization was achieved across the telecom band (1, 540 – 1, 630 nm), with distinct trapping positions directly observed via scattering near-field optical microscopy. The device used complementary metal–oxide–semiconductor-compatible materials, exhibited strong mode confinement and showed robustness to fabrication imperfections, highlighting its practical integration for future multiplexed, on-chip topological photonic devices.

TRT beyond photonics

Although PCs have been a primary platform for TRT, the core principles extend to other wave systems, particularly to acoustic and elastic media. These platforms share the key features of topological protection and slow-light effects. In all three domains (photonic, acoustic and elastic), wave slowing is achieved by engineering the band structure to create flat bands near-zero group velocity. This can result from external gradients (such as refractive index, mass density and stiffness) that create frequency-dependent spatial landscapes or from topological modifications that reshape dispersion without requiring physical gradients. In both cases, robust edge or corner states, protected by topological invariants, ensure defect-tolerant and stable localization, which enables practical implementations of TRT across diverse wave platforms.

TRT in acoustic systems

Acoustic metamaterials provide a compelling platform for TRT because they are easy to fabricate and tune. In these systems, TRT harnesses spatial variations in bulk modulus and density, analogous to permittivity and permeability in photonic systems. The governing wave equation, $\nabla \cdot (\rho(r)^{-1}\nabla p(r)) + \frac{\omega^2}{K(r)}p(r) = 0$, describes pressure fluctuations $p(r)$ in a medium with periodic density $\rho(r)$ and bulk modulus $K(r)$, leading to phononic bandgaps similar to those found in PCs[98–100]. Introducing gradients in density or coupling strength alters the local band structure, enabling frequency-dependent localization of sound. Topological features, such as the valley Hall and quantum spin Hall effects, ensure that these localized acoustic modes remain robust against disorder[101,102], making acoustic TRT a powerful and reliable wave-trapping technique[103,104].

Early demonstrations of acoustic rainbow trapping used non-topological structures, such as arrays of grooved rigid bars with linearly increasing groove depths that enabled frequency-selective energy localization[105]. These designs achieved broadband spectral separation but lacked robustness. To improve energy-harvesting performance, gradient phononic crystals with coupled interfaces were developed[64]. As shown in Fig. 5a, simulations and experiments showed strong agreement, confirming the effectiveness of the system. This work used square-lattice phononic crystals composed of polymeric scatterers in air and integrated a piezoelectric film along the graded interface for efficient energy transduction. Broadband TRT was demonstrated over around 4.39–4.86 kHz, with output power enhanced by up to 91%. The spatial separation of trapped modes was achieved by introducing an external gradient via gradual variation of scatterer size along the interface. Robustness against structural disorder was also verified. High-quality topologically protected interface modes, in which adjusting the water height optimized performance[106] (Fig. 5b), achieved further refinement. This simulation-based study introduced a subwavelength acoustic metamaterial with water-filled resonant cavities in a honeycomb lattice. By tuning the water height, topological phase transitions were controlled, enabling robust spatial separation of sound across multiple frequencies in the 1.548–1.562 kHz range, with immunity to defects and sharp bends.

TRT was also extended to a 2D gradient, created using spatially varying scatterer shapes and geometric orientations to control the location of topological edge and corner states in topological phononic crystals. This enabled multidimensional wave trapping[107] (Fig. 5c). The simulated field patterns confirmed discrete corner trapping across 9.687–9.881 kHz.

Recently, acoustic higher-order topological insulators have been used to realize TRT based on corner states. As shown in Fig. 5d, introducing translational deformations into unit cells of a square-lattice sonic crystal achieved frequency-dependent localization[108]. This experimental work demonstrated deep-subwavelength corner modes that were directionally trapped in a multilane configuration over 2.85–3.08 kHz and confirmed them through near-field scanning. The design enabled tight confinement at scales around 21 times smaller than the wavelength, which makes it highly suitable for applications in advanced acoustic devices, sound filtering and energy harvesting.

TRT in elastic systems

In elastic media, mechanical wave propagation is governed by the elastodynamic equation. For isotropic materials, the displacement field $u(r, t)$ satisfies: $\rho\frac{\partial^2 u}{\partial t^2} = (\lambda + 2\mu)\nabla(\nabla \cdot u) - \mu\nabla \times (\nabla \times u)$, in which λ and μ are Lamé parameters, and ρ is the density. In periodic elastic structures, such as phononic plates and elastic metamaterials, this equation gives rise to well-defined band structures[109–111]. TRT in elastic systems is achieved by introducing spatial gradients in parameters such as mass density or stiffness. These variations reshape the local dispersion relation, slow down specific elastic modes and enable frequency-selective localization. Incorporating topological design principles ensures that the resulting trapped modes are robust against structural imperfections. For instance, graded phononic crystals with smoothly varying elastic properties have demonstrated controlled wave confinement. Resonant cavities embedded in such structures further allow fine-tuning of trapped frequencies with topological protection, applicable even for flexural and torsional modes[66]. These capabilities make TRT attractive for vibration isolation and mechanical energy harvesting.

Early demonstrations of elastic TRT focused on 1D and 2D systems[3]. For example, graded Su–Schrieffer–Heeger metawedges — structures with alternating segments of differing geometry — were used to localize different components of broadband Rayleigh waves at distinct positions[3] (Fig. 6a). This simulation-based study achieved spatial separation of Rayleigh wave components over a broad frequency range of 25.45–54.87 kHz. This concept was later extended to crystalline elastic plates with linearly increasing depth profiles[69]. Elastic TRT was experimentally realized using dislocation-engineered phononic crystals with a graded boundary[112] (Fig. 6b). This work introduced a homogeneous dislocation between two topologically distinct domains. The boundary region was gradually tuned via a translation vector applied to one side of the lattice, and the trapped modes were experimentally measured between 73.5 kHz and 78.5 kHz. The technique allowed for continuous modulation of interface group velocities via translation, enhancing the flexibility and configurability of the system.

A significant advance involved the use of HOTCMs in locally resonant elastic metamaterials to achieve multi-frequency trapping

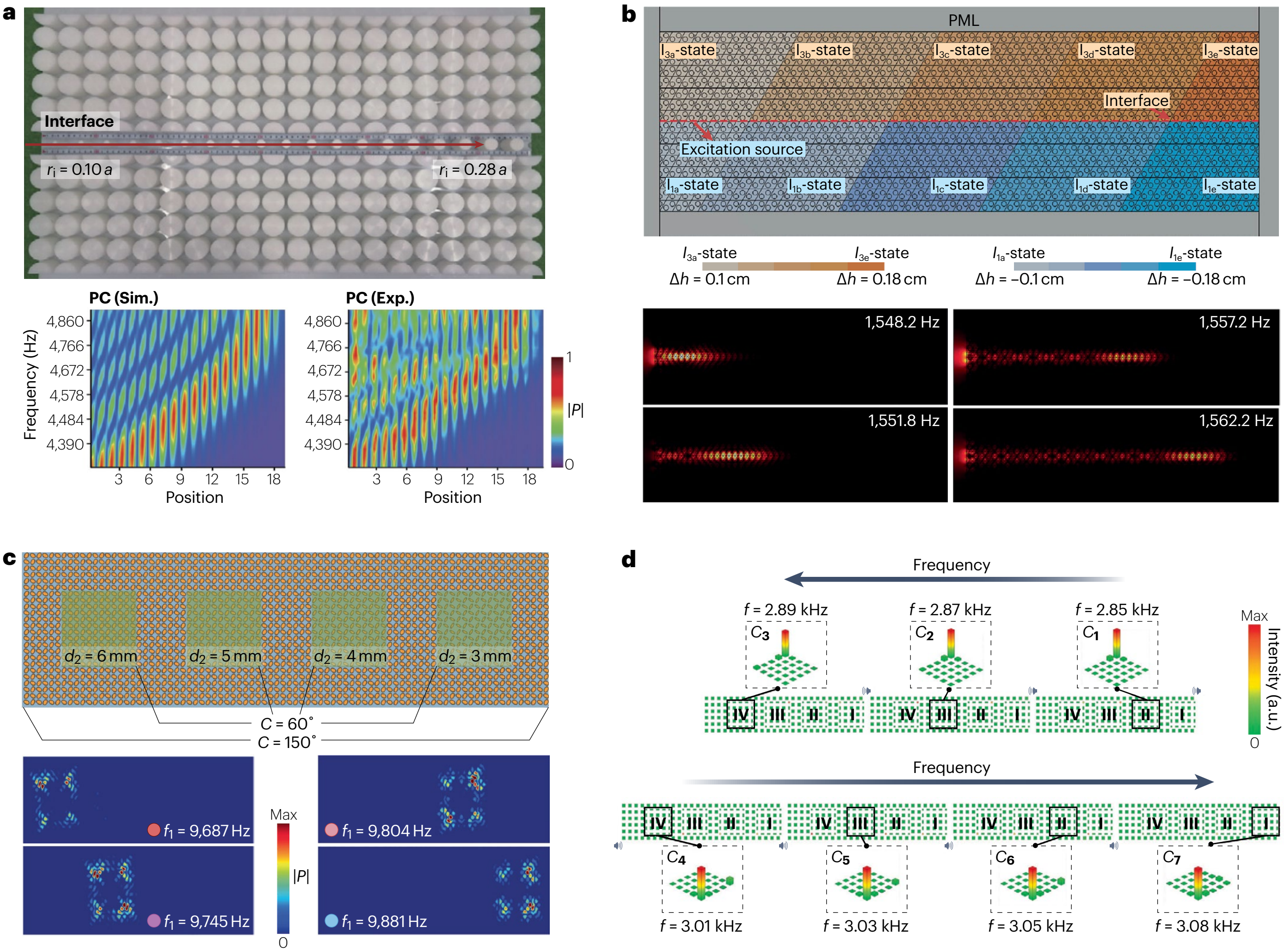

Fig. 5 | Topological rainbow trapping in acoustic systems. a, Gradient phononic crystal designed for acoustic energy harvesting. The structure is fabricated via 3D printing, and the scatterer radius r_i varies progressively from $r_1 = 0.10a$ to $r_2 = 0.28a$, creating an interface gradient that enables frequency-dependent spatial localization, as confirmed in both simulation and experiment. |P| represents pressure field distributions. Adapted with permission from ref. 64, Elsevier. **b**, Topological acoustic waveguide composed of alternating interface states. Domains in blue correspond to I_1-states ($\Delta h < 0$) and those in orange correspond to I_3-states ($\Delta h > 0$), in which Δh denotes the water height variation. The structure is surrounded by perfectly matched layers (PMLs) to avoid wave reflection and ensure accurate simulation results. The two phases are engineered by varying Δh from ±0.1 cm to ±0.18 cm in opposite directions, creating a spatial gradient across the interface to tune the local resonance frequencies. Bottom panels display the corresponding simulated pressure field distributions at different excitation frequencies, in which topological rainbow trapping (TRT) effect is shown. Reprinted with permission from ref. 106, Elsevier. **c**, Simulated acoustic pressure field distributions in a second-order topological sonic crystal formed by integrating four square lattices with side lengths d_2 = 6, 5, 4 and 3 mm. Gradual transitions in topology enable TRT at multiple excitation frequencies, revealing spatially separated corner states. Adapted with permission from ref. 107, Wiley. **d**, Experimental realization of corner-localized TRT in acoustic higher-order topological insulators. Gradual variations in corner geometry across four regions (I–IV) lead to frequency-dependent localization at distinct corner sites (C_1–C_7) observed via pressure field intensity mapping. Reprinted with permission from ref. 108, Elsevier.

at distinct geometric corners[86], as illustrated in Fig. 6c. This experiment demonstrated spatially separated corner modes spanning 1.108–1.302 kHz, with each mode confined to a different corner configuration. Notably, the corner localization was controlled through geometric design, enabling frequency-selective positioning of modes, an important step towards compact, reconfigurable elastic devices.

Finally, in a recent work, TRT was used to develop a piezoelectric meta-device for energy harvesting, incorporating HOTCMs and edge modes to concentrate and convert vibrational energy[113] (Fig. 6d). This experimentally validated design used six topological corners, each supporting distinct resonant frequencies in the range 15.21–16.50 kHz. The vibrational energy at each corner was efficiently converted into electrical output via piezoelectric patches, showcasing a robust and multifunctional platform for high-efficiency energy harvesting based on elastic TRT localization.

Loss mitigation and tuning via complex frequency excitations

Despite the potential of TRT for extreme wave manipulation, two critical challenges for the broad applicability of TRT models are to minimize losses and to attain tunability. Recent advances have enabled rigorous examination of both aspects, particularly in the context of ultrafast applications driven by complex frequency excitations.

Complex frequency excitation refers to an excitation pulse characterized by a complex frequency $\omega = \omega_r + i\omega_i$, in which ω_r is the central (real) frequency of the pulse, and the imaginary frequency ω_i is proportional to the pulse bandwidth[114,115]. Complex frequency excitations interact transiently with materials and can produce a virtual gain effect, causing the system to behave as if it were lossless during the interaction. For example, consider a plasmonic system described by the Drude permittivity $\varepsilon(\omega) = 1 - \omega_p^2/(\omega^2 + i\omega\gamma)$. A complex frequency excitation pulse with frequency $\omega - i\gamma/2$ modifies the permittivity to $\varepsilon(\omega - i\gamma/2) = 1 - \omega_p^2/(\omega^2 + \gamma^2/4)$, in which ω_p is the plasma frequency and γ is the damping rate in the Drude model. That is, the permittivity 'seen' by the pulse is now completely real and loss-free[116,117]. This effect occurs only transiently during the duration of the pulse, and the source supplies the extra energy required to suppress losses. Nevertheless, this does imply that a pulse, such as a Gaussian or exponentially decaying in time, can interact with a plasmonic medium in a completely loss-free manner, as if the plasmonic medium were lossless (virtual gain). In doing so, it effectively restores the zero-group-velocity point that would otherwise be obscured by material losses, which makes this technique especially suitable for ultrafast applications in which interactions are limited to the brief duration of each pulse[118].

Complex frequency-based techniques also enable tunability. The imaginary component ω_i (or γ) allows dynamic tuning of material

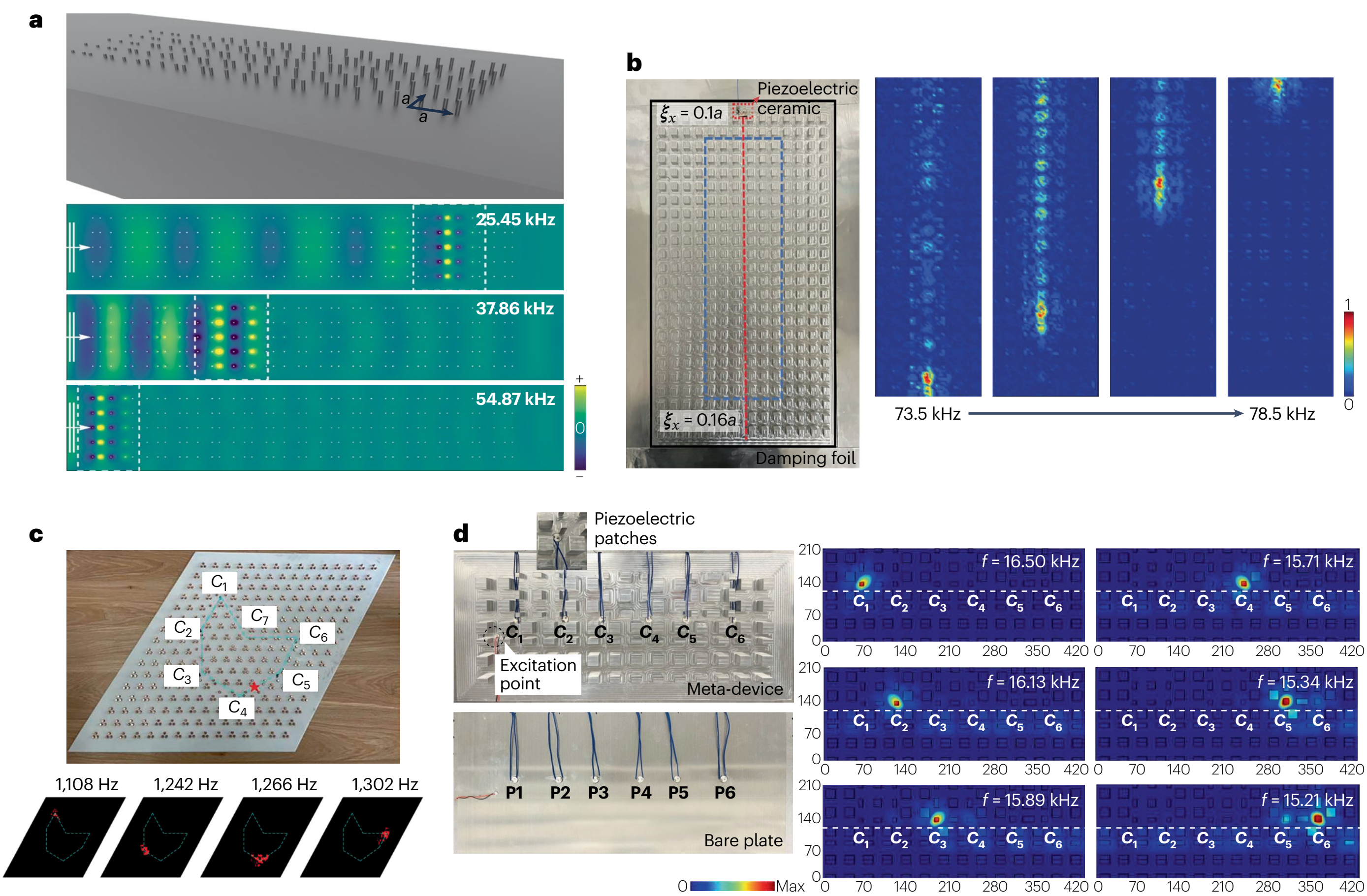

Fig. 6 | Topological rainbow trapping in elastic systems. a, Schematic of a graded Su–Schrieffer–Heeger (SSH) elastic metawedge. The topological rainbow trapping (TRT) effect is achieved by linearly increasing the rod heights from 20 mm to 50 mm (with a being the unit-cell size). Elastic energy localization occurs at distinct spatial locations along the wedge for different excitation frequencies. Adapted with permission from ref. 3, APS. **b**, Experimental setup of an elastic phononic crystal with gradually tuned ξ_x from 0.1a to 0.16a, in which ξ_x refers to the x-component of the 2D translation vector ξ. An ultrasound piezoceramic transducer, acting as an elastic wave source, is placed at one port of the boundary. The blue dashed box indicates the experimental scan area. Out-of-plane displacement fields measured by a scanning laser vibrometer confirm the realization of TRT. Adapted with permission from ref. 112, APS. **c**, Polygonal elastic lattice supporting multiple higher-order topological corner modes (HOTCMs) at different corners C_1–C_7, formed by trivial and nontrivial domains created by locally resonant metamaterial plates. Experimental measurements of out-of-plane displacement fields show frequency-specific confinements of the excited HOTCMs with localized modes sequentially appearing at corners in an anticlockwise order as the excitation frequency increases ($C_1 \rightarrow C_3 \rightarrow C_4 \rightarrow C_6$). Adapted with permission from ref. 86, APS. **d**, Schematics and experimental setup of a fabricated meta-device for elastic wave energy harvesting using HOTCM. Piezoelectric patches (P1–P6) are attached at corner sites C_1–C_6 to convert localized vibrational energy into electrical signals. Laser-scanned out-of-plane displacement fields at different frequencies confirm the frequency-dependent localization of elastic waves TRT. Adapted with permission from ref. 113, Elsevier.

Box 1 | Complex frequency excitations for topological rainbow trapping

Mechanism of virtual gain and localization

Virtual gain temporarily eliminates intrinsic material losses through transient interactions with a propagating wave. Complex frequency excitations provide virtual gain that modifies the response of the system, rendering the medium effectively loss-free during the interaction window with the pulse. This allows energy to concentrate at specific points in space without dissipating prematurely, enabling transient localization. Complex frequency excitations introduce a temporal decay factor to the incoming wave. This can be expressed as $E(t)\alpha\cos(2\pi ft)\ .e^{-\Gamma t}$, in which the decay factor $\Gamma = \omega_i = 2\pi\gamma$, with ω_i representing the imaginary frequency and γ is the decay rate. For a given frequency f, a larger γ leads to faster decay effectively trapping the wave energy near its origin.

Spatial and temporal decay

Spatial localization is influenced by the wavevector **k**, which determines the propagation speed and wavelength of the wave in the medium. For a given spatial position x, the amplitude of the localized wave is determined by $E(x)\alpha e^{-\eta x}$, in which spatial decay constant $\eta = \Gamma/v_g = 2\pi\gamma/v_g$. A higher Γ or lower v_g ($v_g \rightarrow 0$) enhances localization. The spatial localization distance x_{Loc} can be expressed as $x_{Loc} = v_g/\Gamma$. The observed decay is not a result of random loss, but a mechanism for spatially selective energy confinement, leading to concentration rather than dissipation. Unlike traditional losses, in which energy dissipates into the material, this mechanism modifies the amplitude via $e^{-\eta x}$, creating zones of confinement. By tuning γ, frequency-specific localization points can be engineered along the interface. This controlled confinement enables rainbow trapping without a material gradient (see the figure, right panel). By contrast, in gradient-based topological structures, the wave remains localized near the trapped point because the gradient controls energy flow, preventing rapid decay and enabling robust, frequency-selective confinement (see the figure, left panel).

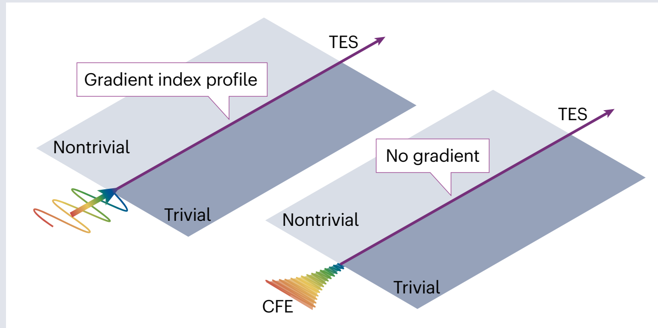

Multiple frequencies (rainbow effect)

Each frequency component decays at its own rate γ_i, resulting in distinct spatial localization points. The amplitude of each component follows $E_i(x)\alpha e^{-\eta_i x}$, in which $\eta_i = \Gamma_i/v_{g,i} = 2\pi\gamma_i/v_{g,i}$. For N frequency components, the total localized wave field $E(x, t) = \sum_{i=1}^{N}\cos(2\pi f_i t)\ .e^{-\Gamma_i t}\ .e^{-\eta_i x}$. Each wave component contributes to the total field with its own temporal decay and spatial localization. Temporal decay ensures that wave energy diminishes over time, but different frequencies decay at different rates, creating temporal separation. Spatial decay, governed by η_i, leads to rainbow trapping. The interplay between group velocity and decay factor determines where and how each frequency localizes along the topological interface, enabling robust, spectrally distinct and spatially separated trapping regions. CFE, complex frequency excitations; TES, topological edge state.

responses without changing the underlying material parameters[119]. For example, by selectively enhancing a multipole term (such as electric dipole and quadrupole), complex frequency excitations can dynamically alter the scattering behaviour. This tunability is achieved by varying γ, which adjusts the strength and interaction of different multipole terms, enabling selective spectral manipulation simply by changing the shape of the incident complex-frequency pulse, rather than altering the material itself.

Combined with topological edge states, complex frequency excitations enable robust frequency-selective localization (Box 1). The imaginary component γ can be engineered to spatially separate different frequency components along the topological interface, effectively realizing a rainbow trapping. This approach achieves robust rainbow trapping purely through temporal wave properties, without altering the physical structure. This dual mechanism – transient loss mitigation and engineered decay – provides precise, tunable and robust control of light trapping in topologically protected systems.

Conclusions and outlook

TRT is an emerging field at the intersection of wave physics, slow light and topology, offering significant opportunities for wave manipulation technologies. By harnessing topological invariants, TRT enables robust, defect-immune confinement and selective frequency localization across a broad spectrum. This Review has outlined the fundamental principles and mechanisms underlying TRT, emphasizing its key distinction from conventional rainbow trapping, namely, its resilience to structural imperfections and scattering. Berry curvature has a pivotal role by introducing an anomalous velocity term, allowing for strong localization even in systems without inherently flat bands.

TRT can be realized through two primary design pathways: applying external gradients to modulate pre-existing topological states and intrinsically engineering topological properties that directly induce near-zero group velocity. These designs are further supported by key implementation frameworks such as graded index profiles, synthetic dimensions and HOTCMs, each facilitating robust and frequency-selective trapping. TRT has been successfully realized in PCs and extended to acoustic and elastic systems, demonstrating its broad applicability. In addition to structural approaches, complex-frequency excitations offer a dynamic way to mitigate losses and enhance tunability, reinforcing the potential of TRT for robust, broadband wave localization in practical systems.

Potential applications

TRT offers a powerful approach to optical filtering by enabling frequency-selective light manipulation. By placing detectors or output couplers at designated locations along a topological interface, specific wavelengths can be spatially extracted with high precision[120]. This makes TRT an ideal platform for applications such as on-chip wavelength division multiplexing[60,121,122] and optical buffering with enhanced efficiency and robustness[123]. Unlike conventional photonic circuits that rely on bulky components that are prone to dispersion-induced signal distortion, TRT achieves frequency separation through spatial localization. This inherent separation reduces crosstalk and interference, even in the presence of fabrication imperfections or scattering[124]. Moreover, by overcoming mode degeneracy, which is common in standard topological waveguides, TRT facilitates efficient wavelength division multiplexing within a single waveguide, streamlining circuit design and reducing device footprint[125]. Additionally, the ability of TRT to control group velocity enables the realization of optical delay lines[126,127], dispersion compensation to align slower and faster channels[75,128] and multichannel optical buffering[56] for improved synchronization in photonic networks. Beyond buffering, TRT can be used to develop high-capacity optical memory devices[129] by encoding information across multiple wavelength channels and leveraging slow-light effects for enhanced storage density. These capabilities position TRT as a promising technology for integrated photonic circuits, which enhances signal processing performance while maintaining compactness and scalability.

In TRT, the combination of slow-light effects and spatial frequency separation significantly enhances light–matter interactions by increasing the interaction time between photons and the material system[130,131]. This enables more efficient nonlinear optical processes, including frequency conversion, second-harmonic generation and four-wave mixing[132,133], as different nonlinear effects can be controlled independently at separate wavelengths. Beyond classical nonlinear optics, TRT facilitates strong photon–photon interactions, making it a promising platform for nonlinear quantum optical devices. By trapping photons at specific spatial locations, TRT enables the wavelength-selective quantum gates, which can manipulate quantum states with high fidelity. For instance, a TRT-based waveguide could support nonlinear interactions at a targeted frequency, while leaving the rest of the spectrum unaffected. This contrasts with conventional topological systems, in which all frequencies may undergo similar nonlinear effects, which limit efficiency. The unique ability of TRT to spatially control nonlinear interactions makes it an effective tool for integrated quantum photonics.

TRT-based structures offer exceptional stability, making them ideal for precision applications such as acoustic rainbow sensors and hearing restoration technologies, in which traditional systems often suffer from signal degradation and crosstalk in the presence of defects. The localized slow-light effect in TRT systems amplifies subtle environmental changes, enabling high-resolution, multi-parameter sensing with enhanced sensitivity[134,135]. Hearing restoration technologies, such as cochlear implants, also benefit from advances in sound processing[136,137]. Incorporating principles akin to acoustic TRT sensors enables the decomposition of complex sound signals into individual frequency components, allowing for more precise auditory nerve stimulation[138]. This may improve sound perception and contribute to a more natural listening experience.

In mechanical systems, the ability of TRT to localize elastic waves at predefined positions improves the accuracy of non-destructive testing by isolating specific vibrational modes, reducing wave dispersion and enhancing damage detection. Additionally, this localized wave confinement enhances mechanical energy harvesting by efficiently concentrating vibrations at targeted locations, eliminating the need for external resonators or frequency-tuning components[139,140]. The combined capabilities of TRT in precise sensing and robust energy harvesting make it highly suitable for applications requiring stability, sensitivity and compact design.

Future research directions

Recent advances in TRT have demonstrated remarkable potential for wave manipulation, but key challenges persist, necessitating a deeper investigation into both theoretical and practical aspects. Hermitian systems offer robust topological protection but often lack the flexibility required for dynamic control. By contrast, non-Hermitian mechanisms introduce new degrees of freedom for manipulating group velocity but can also lead to instabilities arising from gain–loss imbalance or sensitivity near EPs. A key open question is whether Hermitian designs can retain topological robustness while selectively incorporating non-Hermitian features, such as controlled loss gradients and EPs, to enhance tuning capabilities. Developing a systematic framework that balances these strengths is critical for achieving broadband TRT with improved resilience and minimal energy loss.

Another promising direction involves expanding TRT concepts into higher-dimensional synthetic spaces. Existing TRT designs typically extend 2D spatial systems by incorporating one synthetic dimension, forming (2 + 1)D parameter spaces (two spatial dimensions and one synthetic dimension). Exploring configurations involving additional synthetic dimensions, such as (2+2)D or even higher-dimensional synthetic parameter spaces, could unlock richer topological states with enhanced spatial and spectral control. Understanding whether such higher-dimensional synthetic spaces can enable multichannel or multidimensional TRT with improved robustness and functionality is another intriguing research direction.

Integrating TRT principles into plasmonic systems also presents exciting possibilities, as plasmonics inherently support strong field confinement and subwavelength-scale operation. This makes plasmonic platforms ideal candidates to achieve robust, frequency-selective localization in nanoscale environments. Exploring how TRT concepts can extend to topological plasmonics may lead to enhanced sensing technologies and quantum plasmonic devices. Although conventional rainbow trapping has been demonstrated in plasmonic systems, realizing TRT remains challenging owing to intrinsic ohmic losses and because it is difficult to achieve stable topological edge states in a complex, frequency-dependent dispersion. Recent efforts have demonstrated the possibility to sustain topological edge states in lossy plasmonic systems, through the use of compact planar arrays of plasmonic nanoparticles[141], hybrid low-loss platforms[142] and periodically perforated plasmonic waveguides[143]. Continued advances in dispersion control, loss mitigation and interface engineering are steadily bringing TRT in plasmonics closer to practical realization.

Furthermore, integrating TRT with quantum emitter systems offers exciting opportunities for scalable quantum networks and advanced signal control. Zero-group-velocity states of TRT naturally enhance slow-light effects, extending the interaction time between photons and quantum emitters such as quantum dots, diamond defects or atomic systems. This prolonged interaction could enhance coherence, mitigate decoherence effects and improve quantum memory and communication systems[144–146]. Additionally, strong spatial and spectral confinement capabilities of TRT make it well suited for manipulating the quantum states of light. Leveraging these properties may enable improved control over single-photon sources, facilitating precise emission timing and enhanced photon indistinguishability.

Integrating artificial intelligence and machine learning could also improve TRT design by optimizing material compositions and geometries for superior performance. However, further investigation is required to understand how effectively inverse design can be applied to TRT systems to achieve enhanced control, efficiency and robustness.

Recent advances, such as the Landau rainbow, have demonstrated that combining pseudomagnetic and pseudoelectric fields can achieve broadband rainbow trapping by breaking the degeneracy of Landau levels[147]. Meanwhile, the newly proposed continuum Landau mode mechanism leverages non-Hermitian physics through a spatially varying imaginary vector potential to generate a continuous spectrum of localized modes, enabling distortion-free rainbow trapping[148]. Incorporating non-Hermitian elements into these gauge-field designs offers exciting opportunities to improve wave localization precision. Selective damping or amplification of specific Landau modes may enhance frequency separation and control.

Building on earlier demonstrations of on-chip TRT using passive silicon-on-insulator PC waveguides that implement synthetic dimensions for spectral separation[97], recent works[61,149] have extended TRT into the active regime. A notable example is the realization of ultra-compact topological rainbow nanolasers operating in the telecom band, in which a tapered PC nanocavity design supports topologically protected edge modes with diffraction-limited mode volumes and ultra-low thresholds under optical pumping[61]. Although current devices rely on optical pumping, achieving electrical pumping is crucial for fully integrated, energy-efficient multiplexed light sources suitable for scalable on-chip applications. In addition to powering emission, applied electric fields may enable fine spectral tuning of each trapped mode, allowing dynamic modulation and spectral reconfigurability across TRT-enabled devices. Looking ahead, advancing TRT from individual devices to photonic integrated circuits could enable on-chip multiplexed communication, reconfigurable spectral processing and scalable topological photonic networks, in which frequency-separated, robust light channels are dynamically controlled across complex architectures.

Published online: 02 July 2025

References

1. Tsakmakidis, K. L., Boardman, A. D. & Hess, O. 'Trapped rainbow' storage of light in metamaterials. *Nature* **450**, 397–401 (2007).
This landmark work introduces the original concept of rainbow trapping using an axially graded heterostructure incorporating a negative refractive index metamaterial core.
2. Christensen, J., Huidobro, P., Martin-Moreno, L. & Garcia-Vidal, F. Confining and slowing airborne sound with a corrugated metawire. *Appl. Phys. Lett.* **93**, 083502 (2008).
3. Chaplain, G. J., De Ponti, J. M., Aguzzi, G., Colombi, A. & Craster, R. V. Topological rainbow trapping for elastic energy harvesting in graded Su–Schrieffer–Heeger systems. *Phys. Rev. Appl.* **14**, 054035 (2020).
4. Skelton, E., Craster, R., Colombi, A. & Colquitt, D. The multi-physics metawedge: graded arrays on fluid-loaded elastic plates and the mechanical analogues of rainbow trapping and mode conversion. *N. J. Phys.* **20**, 053017 (2018).
5. Wilks, B., Montiel, F. & Wakes, S. Rainbow reflection and broadband energy absorption of water waves by graded arrays of vertical barriers. *J. Fluid Mech.* **941**, A26 (2022).
6. Colombi, A., Colquitt, D., Roux, P., Guenneau, S. & Craster, R. V. A seismic metamaterial: the resonant metawedge. *Sci. Rep.* **6**, 27717 (2016).
7. Krauss, T. F. Slow light in photonic crystal waveguides. *J. Phys. D Appl. Phys.* **40**, 2666–2670 (2007).
8. Krauss, T. F. Why do we need slow light? *Nat. Photon.* **2**, 448 (2008).
This foundational perspective highlights the advantages of slow light.
9. Baba, T. Slow light in photonic crystals. *Nat. Photon.* **2**, 465 (2008).
10. Lu, L., Joannopoulos, J. D. & Soljačić, M. Topological photonics. *Nat. Photon.* **8**, 821–829 (2014).
11. Khanikaev, A. B. & Shvets, G. Two-dimensional topological photonics. *Nat. Photon.* **11**, 763–773 (2017).
12. Ozawa, T. et al. Topological photonics. *Rev. Mod. Phys.* **91**, 015006 (2019).
13. Wang, Q., Xue, H., Zhang, B. & Chong, Y. D. Observation of protected photonic edge states induced by real-space topological lattice defects. *Phys. Rev. Lett.* **124**, 243602 (2020).
14. Peterson, C. W., Li, T., Jiang, W., Hughes, T. L. & Bahl, G. Trapped fractional charges at bulk defects in topological insulators. *Nature* **589**, 376–380 (2021).
15. Noh, J. et al. Topological protection of photonic mid-gap defect modes. *Nat. Photon.* **12**, 408–415 (2018).
16. Noh, J., Huang, S., Chen, K. P. & Rechtsman, M. C. Observation of photonic topological valley Hall edge states. *Phys. Rev. Lett.* **120**, 063902 (2018).
17. Poo, Y., Wu, R.-x, Lin, Z., Yang, Y. & Chan, C. Experimental realization of self-guiding unidirectional electromagnetic edge states. *Phys. Rev. Lett.* **106**, 093903 (2011).
18. Ma, T. & Shvets, G. Scattering-free edge states between heterogeneous photonic topological insulators. *Phys. Rev. B* **95**, 165102 (2017).
19. Xie, B.-Y. et al. Second-order photonic topological insulator with corner states. *Phys. Rev. B* **98**, 205147 (2018).
20. Xie, B.-Y. et al. Visualization of higher-order topological insulating phases in two-dimensional dielectric photonic crystals. *Phys. Rev. Lett.* **122**, 233903 (2019).
21. Li, M. et al. Higher-order topological states in photonic kagome crystals with long-range interactions. *Nat. Photon.* **14**, 89–94 (2020).
22. Wu, L.-H. & Hu, X. Scheme for achieving a topological photonic crystal by using dielectric material. *Phys. Rev. Lett.* **114**, 223901 (2015).
23. Chen, Z.-G. et al. Multiple topological phase transitions in a gyromagnetic photonic crystal. *Phys. Rev. A* **95**, 043827 (2017).
24. Chan, H.-C. & Guo, G.-Y. Tuning topological phase transitions in hexagonal photonic lattices made of triangular rods. *Phys. Rev. B* **97**, 045422 (2018).
25. Bahari, B. et al. Nonreciprocal lasing in topological cavities of arbitrary geometries. *Science* **358**, 636–640 (2017).
26. Mansha, S. & Chong, Y. D. Robust edge states in amorphous gyromagnetic photonic lattices. *Phys. Rev. B* **96**, 121405 (2017).
27. Ma, H., Ju, C., Xi, X. & Wu, R.-X. Nonreciprocal Goos–Hänchen shift by topological edge states of a magnetic photonic crystal. *Opt. Exp.* **28**, 19916–19925 (2020).
28. Wang, Z., Chong, Y., Joannopoulos, J. D. & Soljačić, M. Observation of unidirectional backscattering-immune topological electromagnetic states. *Nature* **461**, 772–775 (2009).
29. Longhi, S., Gatti, D. & Valle, G. D. Robust light transport in non-Hermitian photonic lattices. *Sci. Rep.* **5**, 13376 (2015).
30. Shalaev, M. I., Walasik, W., Tsukernik, A., Xu, Y. & Litchinitser, N. M. Robust topologically protected transport in photonic crystals at telecommunication wavelengths. *Nat. Nanotechnol.* **14**, 31–34 (2019).
31. Xiao, D., Chang, M.-C. & Niu, Q. Berry phase effects on electronic properties. *Rev. Mod. Phys.* **82**, 1959–2007 (2010).
32. Bliokh, K. Y. & Bliokh, Y. P. Spin gauge fields: from Berry phase to topological spin transport and Hall effects. *Ann. Phys.* **319**, 13–47 (2005).
33. Thouless, D. J., Kohmoto, M., Nightingale, M. P. & den Nijs, M. Quantized Hall conductance in a two-dimensional periodic potential. *Phys. Rev. Lett.* **49**, 405 (1982).
34. Wang, H.-X., Guo, G.-Y. & Jiang, J.-H. Band topology in classical waves: Wilson-loop approach to topological numbers and fragile topology. *N. J. Phys.* **21**, 093029 (2019).
35. Wang, C., Zhang, H., Yuan, H., Zhong, J. & Lu, C. Universal numerical calculation method for the Berry curvature and Chern numbers of typical topological photonic crystals. *Front. Optoelectron.* **13**, 73–88 (2020).
36. Karplus, R. & Luttinger, J. Hall effect in ferromagnetics. *Phys. Rev.* **95**, 1154 (1954).
37. Chang, M.-C. & Niu, Q. Berry phase, hyperorbits, and the Hofstadter spectrum. *Phys. Rev. Lett.* **75**, 1348 (1995).
38. Price, H. M. & Cooper, N. R. Effects of Berry curvature on the collective modes of ultracold gases. *Phys. Rev. Lett.* **111**, 220407 (2013).
39. Łempicka-Mirek, K. et al. Electrically tunable Berry curvature and strong light–matter coupling in liquid crystal microcavities with 2D perovskite. *Sci. Adv.* **8**, eabq7533 (2022).
40. Alon, B., Ilan, R. & Goldstein, M. Quantum metric dependent anomalous velocity in systems subject to complex electric fields. *Phys. Rev. B* **110**, 245103 (2024).
41. Price, H. M. & Cooper, N. Mapping the Berry curvature from semiclassical dynamics in optical lattices. *Phys. Rev. A* **85**, 033620 (2012).
42. Zhou, J., Shan, W.-Y., Yao, W. & Xiao, D. Berry phase modification to the energy spectrum of excitons. *Phys. Rev. Lett.* **115**, 166803 (2015).
43. Ge, J. et al. Unconventional Hall effect induced by Berry curvature. *Nat. Sci. Rev.* **7**, 1879–1885 (2020).
44. Jungwirth, T., Niu, Q. & MacDonald, A. Anomalous Hall effect in ferromagnetic semiconductors. *Phys. Rev. Lett.* **88**, 207208 (2002).
45. Fang, Z. et al. The anomalous Hall effect and magnetic monopoles in momentum space. *Science* **302**, 92–95 (2003).
46. Murakami, S., Nagaosa, N. & Zhang, S.-C. Dissipationless quantum spin current at room temperature. *Science* **301**, 1348–1351 (2003).
47. Sundaram, G. & Niu, Q. Wave-packet dynamics in slowly perturbed crystals: gradient corrections and Berry-phase effects. *Phys. Rev. B* **59**, 14915 (1999).
48. Adams, E. & Blount, E. Energy bands in the presence of an external force field — II: anomalous velocities. *J. Phys. Chem. Solids* **10**, 286–303 (1959).
49. Onoda, M., Murakami, S. & Nagaosa, N. Hall effect of light. *Phys. Rev. Lett.* **93**, 083901 (2004).
50. Wimmer, M., Price, H. M., Carusotto, I. & Peschel, U. Experimental measurement of the Berry curvature from anomalous transport. *Nat. Phys.* **13**, 545–550 (2017).
51. Hasan, M. Z. & Kane, C. L. Colloquium: topological insulators. *Rev. Mod. Phys.* **82**, 3045–3067 (2010).
52. Moore, J. E. The birth of topological insulators. *Nature* **464**, 194–198 (2010).

53. Lu, L., Joannopoulos, J. D. & Soljačić, M. Topological states in photonic systems. *Nat. Phys.* **12**, 626–629 (2016).
54. Vlasov, Y. A., O'Boyle, M., Hamann, H. F. & McNab, S. J. Active control of slow light on a chip with photonic crystal waveguides. *Nature* **438**, 65 (2005).
55. Tanabe, T., Notomi, M., Kuramochi, E., Shinya, A. & Taniyama, H. Trapping and delaying photons for one nanosecond in an ultrasmall high-Q photonic-crystal nanocavity. *Nat. Photon.* **1**, 49–52 (2007).
56. Elshahat, S., Wang, C., Zhang, H. & Lu, C. Perspective on the topological rainbow. *Appl. Phys. Lett.* **119**, 230505 (2021).
57. Chen, J., Liang, W. & Li, Z.-Y. Switchable slow light rainbow trapping and releasing in strongly coupling topological photonic systems. *Photon. Res.* **7**, 1075–1080 (2019).
This early work demonstrates topological rainbow trapping in a magneto-optical photonic crystal waveguide.
58. Lu, C., Wang, C., Xiao, M., Zhang, Z. Q. & Chan, C. T. Topological rainbow concentrator based on synthetic dimension. *Phys. Rev. Lett.* **126**, 113902 (2021).
This work introduces the concept of a topological rainbow concentrator using synthetic dimension.
59. Zhang, W.-J., Mo, H.-C., Chen, W.-J., Chen, X.-D. & Dong, J.-W. Observation of gapless corner modes of photonic crystal slabs in synthetic translation dimensions. *Photon. Res.* **12**, 444–455 (2024).
60. Ma, J. et al. Asymmetric frequency multiplexing topological devices based on a floating edge band. *Photon. Res.* **12**, 1201–1212 (2024).
61. Tian, F. et al. Ultra-compact topological photonic crystal rainbow nanolasers operating in the 1550 nm telecom band with wavelength-scale mode volumes. Preprint at https://arxiv.org/abs/2411.11009 (2024).
This work experimentally demonstrates ultra-compact topological photonic crystal rainbow nanolasers operating in the telecom band.
62. Zhang, Z.-D., Yu, S.-Y., Lu, M.-H. & Chen, Y.-F. Gigahertz surface acoustic wave topological rainbow in nanoscale phononic crystals. *Phys. Rev. Lett.* **133**, 267001 (2024).
63. Li, Y. & Li, J. Bidirectional gradient acoustic enhancement and collection based on the dual edge states. *Appl. Acoust.* **236**, 110716 (2025).
64. Tang, X.-L., Ma, T.-X., Kim, M. & Wang, Y.-S. Topological rainbow trapping and broadband piezoelectric energy harvesting of acoustic waves in gradient phononic crystals with coupled interfaces. *Appl. Acoust.* **233**, 110630 (2025).
65. Chen, K., Dong, X., Peng, Z. & Meng, G. Reconfigurable topological gradient metamaterials and potential applications. *Thin-Walled Struct.* **205**, 112572 (2024).
66. Yuan, W. et al. Topological rainbow trapping, concentration and guiding in graded elastic valley phononic crystal plate. *Eng. Struct.* **304**, 117596 (2024).
67. Yan, L., Guo, Z., Chen, Y. & Liu, Y. Functionally graded elastic valley metamaterials for low-frequency surface wave manipulation. *Mech. Adv. Mater. Struct.* https://doi.org/10.1080/15376494.2024.2433695 (2024).
68. Lu, C. et al. Observation of topological rainbow in non-Hermitian systems. *Chin. Opt. Lett.* **21**, 123601 (2023).
69. Ungureanu, B., Makwana, M. P., Craster, R. V. & Guenneau, S. Localizing elastic edge waves via the topological rainbow effect. *Phys. Rev. Appl.* **15**, 014057 (2021).
This early work introduces the topological rainbow effect in elastic systems by combining valley-Hall states and geometric grading.
70. Fang, H., Xie, G., Huang, H. & Chen, J. Coupled topological rainbow trapping of elastic waves in two-dimensional phononic crystals. *Sci. Rep.* **14**, 17011 (2024).
71. Skirlo, S. A. et al. Experimental observation of large Chern numbers in photonic crystals. *Phys. Rev. Lett.* **115**, 253901 (2015).
72. Skirlo, S. A., Lu, L. & Soljačić, M. Multimode one-way waveguides of large Chern numbers. *Phys. Rev. Lett.* **113**, 113904 (2014).
73. Joannopoulos, J. D., Johnson, S. G., Winn, J. N. and Meade, R. D. *Photonic Crystals: Molding the Flow of Light* (Princeton Univ. Press, 2008).
74. Liu, J., Lu, X., Dai, X. & Xiang, Y. Rainbow trapping and releasing based on the topological photonic crystals and a gradient 1D array. *J. Appl. Phys.* **132**, 173105 (2022).
75. Zhang, H., Gao, J. & Xiong, D. Realization of topological fast and slow light based on gradient sandwich structure. *Opt. Exp.* **32**, 46849–46861 (2024).
76. AbdelAll, N., Almokhtar, M., Khouqeer, G. & Soliman, S. E. Realizing the topological rainbow based on cavity-coupled topological edge state. *Opt. Laser Technol.* **171**, 110351 (2024).
77. Guan, A.-Y. et al. Controlling sound wave propagation in topological crystalline insulators and rainbow-trapping. *Phys. Rev. Appl.* **18**, 044054 (2022).
This work demonstrates broadband acoustic rainbow trapping by tuning the surface impedances of topological crystalline insulators.
78. Wu, B., Wang, T., Li, S. & Ma, T. Tunable acoustic energy concentrations based on pseudo-spin locking waveguides and topological rainbow trappings. Preprint at https://arxiv.org/abs/2412.02463 (2024).
79. Sun, X.-W. et al. Sub-wavelength topological boundary states and rainbow trapping of local-resonance phononic crystal plate. *J. Phys. D Appl. Phys.* **57**, 225302 (2024).
80. Zhang, H. et al. Topological rainbow based on graded topological photonic crystals. *Opt. Lett.* **46**, 1237–1240 (2021).
81. Li, M. X., Wang, Y. K., Lu, M. J. & Sang, T. Dual-mode of topological rainbow in gradual photonic heterostructures. *J. Phys. D Appl. Phys.* **55**, 095103 (2022).
82. Mao, Y., Li, Z., Hu, W., Dai, X. & Xiang, Y. Topological slow light rainbow trapping and releasing based on gradient valley photonic crystal. *J. Lightwave Technol.* **40**, 5152–5156 (2022).
83. Elshahat, S., Zhang, H. & Lu, C. Topological rainbow based on coupling of topological waveguide and cavity. *Opt. Exp.* **31**, 20187–20199 (2023).
84. Goldzak, T., Mailybaev, A. A. & Moiseyev, N. Light stops at exceptional points. *Phys. Rev. Lett.* **120**, 013901 (2018).
85. Ding, K., Fang, C. & Ma, G. Non-Hermitian topology and exceptional-point geometries. *Nat. Rev. Phys.* **4**, 745–760 (2022).
86. Zhou, L. & Yu, W. Visualization of rainbow trapping effect in higher-order topological insulators. *Phys. Rev. B* **107**, 174105 (2023).
87. Liang, L. et al. Rainbow trapping based on higher-order topological corner modes. *Opt. Lett.* **47**, 1454–1457 (2022).
This work proposes a new rainbow trapping mechanism based on higher-order topological corner modes.
88. AbdelAll, N., Almokhtar, M., Khouqeer, G., Abood, I. & El. Soliman, S. Rainbow trapping with engineered topological corner states and cavities in photonic crystals. *Adv. Quantum Technol.* **7**, 2400050 (2024).
89. Schindler, F. et al. Higher-order topological insulators. *Sci. Adv.* **4**, eaat0346 (2018).
90. Xie, B. et al. Higher-order band topology. *Nat. Rev. Phys.* **3**, 520–532 (2021).
91. Benalcazar, W. A., Li, T. & Hughes, T. L. Quantization of fractional corner charge in C_n-symmetric higher-order topological crystalline insulators. *Phys. Rev. B* **99**, 245151 (2019).
92. Takahashi, R., Zhang, T. & Murakami, S. General corner charge formula in two-dimensional C_n-symmetric higher-order topological insulators. *Phys. Rev. B* **103**, 205123 (2021).
93. Yuan, L., Lin, Q., Xiao, M. & Fan, S. Synthetic dimension in photonics. *Optica* **5**, 1396–1405 (2018).
94. Nakata, Y., Ito, Y., Nakamura, Y. & Shindou, R. Topological boundary modes from translational deformations. *Phys. Rev. Lett.* **124**, 073901 (2020).
95. Lustig, E. & Segev, M. Topological photonics in synthetic dimensions. *Adv. Opt. Photon.* **13**, 426–461 (2021).
96. Zhao, W., Zheng, Y. & Lu, C. Topological rainbow trapping based on non-Hermitian twisted piecing photonic crystals. *Photon. Res.* **10**, 2728–2733 (2022).
97. Lu, C. et al. On-chip nanophotonic topological rainbow. *Nat. Commun.* **13**, 2586 (2022).
This experimental work demonstrates a topological rainbow effect integrated on a silicon photonic chip.
98. Elmore, W. C. & Heald, M. A. *Physics of Waves* (Dover Publications, 1985).
99. Kushwaha, M. S., Halevi, P., Dobrzynski, L. & Djafari-Rouhani, B. Acoustic band structure of periodic elastic composites. *Phys. Rev. Lett.* **71**, 2022–2025 (1993).
100. Meyer, E. *Physical and Applied Acoustics: An Introduction* (Academic Press, 2012).
101. Xue, H., Yang, Y. & Zhang, B. Topological acoustics. *Nat. Rev. Mater.* **7**, 974–990 (2022).
102. Yves, S., Fleury, R., Lemoult, F., Fink, M. & Lerosey, G. Topological acoustic polaritons: robust sound manipulation at the subwavelength scale. *N. J. Phys.* **19**, 075003 (2017).
103. Tian, Z. et al. Dispersion tuning and route reconfiguration of acoustic waves in valley topological phononic crystals. *Nat. Commun.* **11**, 762 (2020).
104. Wang, Z. et al. Probing two distinct types of topological rainbow concentrators related to the acoustic valley Hall insulator in synthesized three-dimensional space. *Phys. Rev. Appl.* **17**, 064002 (2022).
105. Zhu, J. et al. Acoustic rainbow trapping. *Sci. Rep.* **3**, 1728 (2013).
106. Wang, G., Wei, Y., Chen, Z. & Lim, C. W. Controllable subwavelength topological rainbow trapping in water-filling acoustic metamaterials. *Appl. Acoust.* **207**, 109366 (2023).
107. Chen, J. J., Yang, Q. S., Huo, S. Y. & Fu, C. M. Multidimensional rainbow trapping of sound in the second-order topological sonic crystals. *Phys. Stat. Sol. B* **261**, 2400200 (2024).
108. Liao, D. et al. Synthesizing topological acoustic rainbow trapping at deep-subwavelength corners. *Sci. Bull.* **68**, 1744–1747 (2023).
109. Röhlig, D., Kuhn, E., Teichert, F., Thränhardt, A. & Blaudeck, T. Function phononic crystals. *Europhys. Lett.* **145**, 26001 (2024).
110. Sigalas, M. & Economou, E. N. Band structure of elastic waves in two dimensional systems. *Solid State Commun.* **86**, 141–143 (1993).
111. Demanet, L. *Waves and Imaging: Class Notes* — 18.367 (Massachusetts Institute of Technology, 2017).
112. Zhang, Z.-D. et al. Homogeneous dislocation-induced rainbow concentrating for elastic waves. *Phys. Rev. Appl.* **18**, 044015 (2022).
113. Chen, Y., Fan, L., Zhu, J., An, L. & Su, Z. Rainbow energy harvesting using a high-order topological meta-device. *Nano Energy* **127**, 109722 (2024).
This experimental work pioneers a topological meta-device for rainbow energy harvesting in phononic insulators.
114. Tsakmakidis, K. L., Pickering, T. W., Hamm, J. M., Page, A. F. & Hess, O. Completely stopped and dispersionless light in plasmonic waveguides. *Phys. Rev. Lett.* **112**, 167401 (2014).
115. Tsakmakidis, K. L., Baskourelos, K. G. & Wartak, M. S. *Metamaterials and Nanophotonics: Principles, Techniques and Applications* (World Scientific, 2022).
116. Guan, F. et al. Overcoming losses in superlenses with synthetic waves of complex frequency. *Science* **381**, 766–771 (2023).
117. Kim, S., Peng, Y.-G., Yves, S. & Alù, A. Loss compensation and superresolution in metamaterials with excitations at complex frequencies. *Phys. Rev. X* **13**, 041024 (2023).
118. Tsakmakidis, K. L., Baskourelos, K. & Stefański, T. Topological, nonreciprocal, and multiresonant slow light beyond the time-bandwidth limit. *Appl. Phys. Lett.* **119**, 190501 (2021).
119. Zouros, G. P., Loulas, I., Almpanis, E., Krasnok, A. & Tsakmakidis, K. L. Anisotropic virtual gain and large tuning of particles' scattering by complex-frequency excitations. *Commun. Phys.* **7**, 283 (2024).
This work introduces anisotropic virtual gain to control scattering via complex-frequency excitations.
120. Liu, M.-D. et al. On-chip topological photonic crystal nanobeam filters. *Nano Lett.* **24**, 1635–1641 (2024).

121. Yan, Q., Ma, R., Lyu, Q., Hu, X. & Gong, Q. Transmissible topological edge states based on Su–Schrieffer–Heeger photonic crystals with defect cavities. *Nanophotonics* **13**, 1397–1406 (2024).
122. Wu, Z. et al. Elastic wave demultiplexer with frequency dependent topological valley Hall edge states. *Thin-Walled Struct.* **201**, 111997 (2024).
123. Wu, Y. et al. Applications of topological photonics in integrated photonic devices. *Adv. Opt. Mater.* **5**, 1700357 (2017).
124. Tang, G., Huang, Y., Chen, J., Li, Z.-Y. & Liang, W. A topological multichannel add-drop filter based on gyromagnetic photonic crystals. *Nanomaterials* **13**, 1711 (2023).
125. Elshahat, S., Esmail, M. S. M., Yuan, H., Feng, S. & Lu, C. Broadband multiple topological rainbows. *Ann. Phys.* **534**, 2200137 (2022).
126. Hafezi, M., Demler, E. A., Lukin, M. D. & Taylor, J. M. Robust optical delay lines with topological protection. *Nat. Phys.* **7**, 907–912 (2011).
127. Zhang, Z. et al. Topological acoustic delay line. *Phys. Rev. Appl.* **9**, 034032 (2018).
128. Zhang, Z. et al. Observation of spatiotemporal dynamics for topological surface states with on-demand dispersion. *Photon. Res.* **12**, 2919–2930 (2024).
129. Li, X.-X., Wang, J.-X., Chen, Y.-H. & Zhang, X. Topologically protected spatial-phase mismatching for cavity-enhanced quantum memories. *Phys. Rev. A* **109**, 043511 (2024).
130. Arregui, G., Gomis-Bresco, J., Sotomayor-Torres, C. M. & Garcia, P. D. Quantifying the robustness of topological slow light. *Phys. Rev. Lett.* **126**, 027403 (2021).
This work quantifies how disorder impacts slow light in topological waveguides.
131. Goban, A. et al. Atom–light interactions in photonic crystals. *Nat. Commun.* **5**, 3808 (2014).
132. Kang, M., Liu, T., Chan, C. & Xiao, M. Applications of bound states in the continuum in photonics. *Nat. Rev. Phys.* **5**, 659–678 (2023).
133. Zalogina, A. et al. High-harmonic generation from a subwavelength dielectric resonator. *Sci. Adv.* **9**, eadg2655 (2023).
134. Karlos, A. & Elliott, S. J. Cochlea-inspired design of an acoustic rainbow sensor with a smoothly varying frequency response. *Sci. Rep.* **10**, 10803 (2020).
135. Zhao, L. & Zhou, S. Compact acoustic rainbow trapping in a bioinspired spiral array of graded locally resonant metamaterials. *Sensors* **19**, 788 (2019).
136. Briggs, R. J. Future technology in cochlear implants: assessing the benefit. *Cochlear Implant Int.* **12**, S22–S25 (2011).
137. Kulkarni, K. & Hartley, D. E. Recent advances in hearing restoration. *J. R. Soc. Med.* **101**, 116–124 (2008).
138. Li, Z. et al. Study on recovery strategy of hearing loss & SGN regeneration under physical regulation. *Adv. Sci.* **12**, 2410919 (2025).
139. De Ponti, J. M. *Graded Elastic Metamaterials for Energy Harvesting* (Springer, 2021).
140. Li, J., Tang, H. & Chen, Y. Electro-mechanical multi-branch channel driven by higher-order topological rainbow. *Mech. Adv. Mater. Struct.* https://doi.org/10.1080/15376494.2025.2468378 (2025).
141. Honari-Latifpour, M. & Yousefi, L. Topological plasmonic edge states in a planar array of metallic nanoparticles. *Nanophotonics* **8**, 799–806 (2019).
142. Lin, S. & Wong, Z. J. Hybrid plasmonic valley-Hall topological insulators. *Nanophotonics* **13**, 2811–2817 (2024).
143. Gladstein Gladstone, R., Dev, S., Allen, J., Allen, M. & Shvets, G. Topological edge states of a long-range surface plasmon polariton at the telecommunication wavelength. *Opt. Lett.* **47**, 4532–4535 (2022).
144. Heinrich, A. J. et al. Quantum-coherent nanoscience. *Nat. Nanotechnol.* **16**, 1318–1329 (2021).
145. Lu, C.-C. et al. On-chip topological nanophotonic devices. *Chip* **1**, 100025 (2022).
146. Biswas, S., De, A. & Dutt, A. Topological argument for robustness of coherent states in quantum optics. Preprint at https://arxiv.org/abs/2409.12292 (2024).
147. Zhao, W. et al. Landau rainbow induced by artificial gauge fields. *Phys. Rev. Lett.* **133**, 233801 (2024).
148. Wang, Q. et al. Continuum of bound states in a non-Hermitian model. *Phys. Rev. Lett.* **130**, 103602 (2023).
149. Wang, C. et al. Programmable rainbow-colored optofluidic fiber laser encoded with topologically structured chiral droplets. *ACS Nano* **15**, 11126–11136 (2021).

Acknowledgements
M.B. and K.L.T. acknowledge funding within the framework of the National Recovery and Resilience Plan Greece 2.0, funded by the European Union NextGenerationEU (Implementation body: HFRI), under grant no. 16909. K.L.T. was also supported by the General Secretariat for Research and Technology and the Hellenic Foundation for Research and Innovation under grant no. 4509. S.E.S. and Z.J.W. acknowledge funding from the Ningbo Yongjiang Talent Program (2022A-241-G).

Author contributions
S.E.S., Z.J.W. and K.L.T. researched data for the article. S.E.S., M.B., Z.J.W. and K.L.T. contributed substantially to discussion of the content. S.E.S., Z.J.W. and K.L.T. wrote the article. S.E.S., Z.J.W. and K.L.T. reviewed and/or edited the manuscript before submission.

Competing interests
The authors declare no competing interests.

Additional information
Peer review information *Nature Reviews Physics* thanks Johan Christensen, Yuanjian Xiang and the other, anonymous, reviewer(s) for their contribution to the peer review of this work.

Publisher's note Springer Nature remains neutral with regard to jurisdictional claims in published maps and institutional affiliations.